Coordination Chemistry Reviews 253 (2009) 687–703

Contents lists available at ScienceDirect

Coordination Chemistry Reviews

journal homepage: www.elsevier.com/locate/ccr

Review

Understanding the M–(NHC) (NHC = N-heterocyclic carbene) bond

Heiko Jacobsen [a], Andrea Correa [b], Albert Poater [b], Chiara Costabile [b], Luigi Cavallo [b,*]

[a] KemKom, 1215 Ursulines Avenue, New Orleans, LA 70116, USA
[b] Dipartimento di Chimica, Università di Salerno, Via ponte don Melillo, I-84084 Fisciano (SA), Italy

Contents

ARTICLE INFO

Article history:
Received 18 March 2008
Accepted 10 June 2008
Available online 20 June 2008

Keywords:
N-heterocyclic carbenes
Transition metals
M—ligand bond
DFT methods

ABSTRACT

N-heterocyclic carbenes (NHC) is a well established class of new ligands in organometallic chemistry. Their use as ligands in many reactions catalyzed by transition metal complexes has stimulated intensive research to understand the unique features of the M—(NHC) bond. This review is aimed to provide an overview of the main contributions achieved by the application of advanced computational techniques.

* Corresponding author.
E-mail address: lcavallo@unisa.it (L. Cavallo).

0010-8545/$ – see front matter © 2008 Elsevier B.V. All rights reserved.
doi:10.1016/j.ccr.2008.06.006

1. Introduction

It is the time to promove N-heterocyclic carbenes (NHC) from the status of "emerging alternative to ubiquitous phosphines" to the higher status of "well established ligands in catalysis". Indeed, complexes of transition metals containing NHC ligands can be purchased on the web from well established chemical suppliers. The existence of stable NHCs was intuited by Wanzlick et al. at the beginning of the 1960s [1,2] and supported by the first independent reports by Öfele and Wanzlick of transition metal complexes containing NHC ligands around 1970 [3–5].

However, no diaminocarbene had been isolated with relatively high stability, i.e. without tendency to dimerize [6,7] until the milestone report of Arduengo et al. of a stable crystalline carbene in 1991 [6]. The first stable NHC was based on the imidazol-2-ylidene ring and had adamantyl groups as substituents on the N atoms (IAd in Chart 1), enjoying thermodynamic as well as kinetic stability in the absence of oxygen and moisture [6]. The steric hindrance of the adamantyl groups plays a key role, protecting the free NHC from dimerization. Subsequently, the 1,3-dimethylimidazol-2-ylidene (IMe in Chart 1) and the 1,3,4,5-tetramethylimidazol-2-ylidene (ITM in Chart 1) NHCs were synthesized, although they revealed to be unstable when pure, and were not crystallized but characterized as an oil [8]. Replacement of the alkyl substituents on the N atoms with simple aromatic substituents did not allow isolating free NHCs. However, the introduction of methyl or chloride groups on the aromatic substituents stabilized three new NHCs, 1,3-bis(2,4,6-trimethylphenyl)imidazol-2-ylidene (IMes in Chart 1), 1,3-bis(4-methylphenyl)imidazol-2-ylidene (ITol in Chart 1), and 1,3-bis(4-chlorophenyl)imidazol-2-ylidene [8]. The substitution of the hydrogens at the C4 and C5 atoms of the imidazole ring of IMes by chlorides resulted in an extraordinarily air stable NHC [9]. This remarkable stability was explained through a π-electron donating effect of the Cl lone pairs and to a σ-electron withdrawing effect due to the high electronegativity of the Cl atoms, which reduces and thus stabilizes the basicity of the σ-lone pair at the carbene center. Furthermore, the isolation of NHCs with N-substituents far less bulky than adamantyl, clearly indicated that steric hindrance is not the only factor explaining the stability of the first NHC isolated by Arduengo. Indeed, adequate electronic stabilization of the carbene center in imidazol-2-ylidenes is enough to isolate free NHCs even in the absence of steric protection.

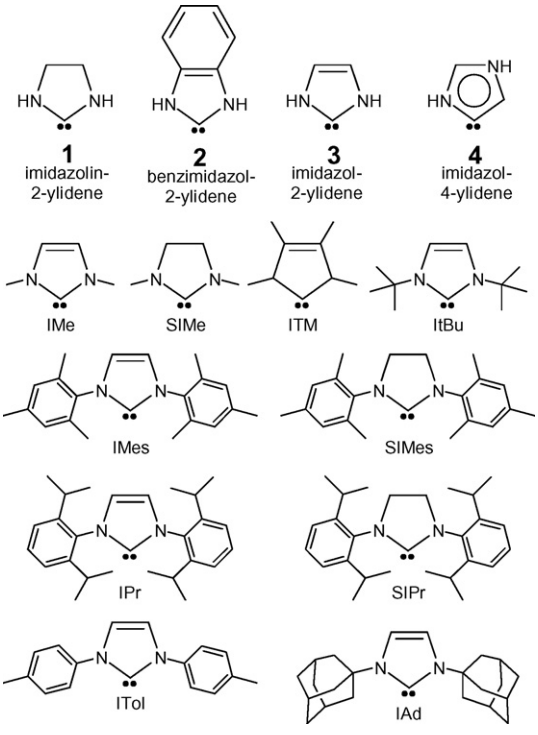

Chart 1.

Until 1995 the C=C double bond of the imidazol-2-ylidene ring was supposed to be a required structural feature for the stability of free NHC. However, another milestone report by Arduengo, the isolation of the first NHC with a saturated imidazolin-2-ylidene ring (SIMes in Chart 1), broke this paradigma [10]. The saturation of the C4=C5 double bond of the imidazol ring does not change the structure of the resulting NHC sensibly. Among the small structural changes due to the σ-effects are an increase in the N–C–N angle, and a slight elongation of C—N bond.

The discovery of stable NHCs of course opened the route to an explosion of studies devoted to the synthesis of new NHCs, to their characterization, and to their use as ligands in transition metal complexes. The nice surprise was that NHCs ligands could easily replace phosphines, and that NHC-based catalysts were very stable under many catalytic conditions, although they present a carbene functionality. This ability initiated impressive academic and industrial efforts, and as a result a great number of effective NHC-bearing catalysts with very different structures have been designed. In many cases these catalysts exhibited better activity than the corresponding phosphine-based catalysts, the most noticeable example are in the field of Ru-catalyzed metathesis of olefins [11–17], Ir-catalyzed hydrogenation [18–20], Pd-catalyzed C—C coupling rections [21–23], and/or led to unexpected reactivity, as in the case of Au-catalyzed reactions [24,25]. Further, H atoms in positions 4, 5 of the saturated imidazolin-2-ylidene ring is a key structural feature for the introduction of asymmetry in the NHC ring, which opens the door to the use of chiral NHCs in asymmetric synthesis [14,26–29].

The importance that NHCs ligands have acquired in practical applications spurred a remarkable amount of work focused on the understanding of M—(NHC) bond from an experimental and a theoretical point of view. The three orbital contributions to the M—(NHC) bond are shown in Fig. 1. The starting hypothesis that NHCs were simple σ-donors is now abandoned, while it is clear that both $d \rightarrow \pi^*$ M to NHC π^*-backdonation as well as $\pi \rightarrow d$ NHC to M π-donation have to be considered to understand the details of the M—(NHC) bond. These contributions also depends on the nature of the NHC skeleton, and it is well accepted that saturated NHCs based on the imidazolin-2-ylidene skeleton **1** of Chart 1, are more basic than NHCs with an aromatic ring fused on the NHC ring, such as the benzimidazol-2-ylidene skeleton **2** of Chart 1, and the unsaturated NHCs based on the imidazol-2-ylidene skeleton **3** of Chart 1. This variation of the NHC skeleton, associated with variation of the N-bonded substituents allows for a tuning of the electronic properties of the specific NHC ligand. On the other hand, in strict similarity with phosphines appropriate selection of the N-bonded R substituents proved very effective in a variation of the steric hindrance of NHC ligand. Thus, NHCs are ligands that allow for a remarkable diversity in the steric and electronic properties, which can be tuned almost at wish.

In this review, which is not exhaustive, we will report on the fundamental insights that the theoretical community has contributed to improve our understanding of the stability of free NHCs, and of the electronic and steric factors associated with the stability of the M—(NHC) bond. To link the theoretical results to the experimental advances in the field, we will also discuss a tiny fraction of the huge amount of experiments that have been performed. Finally, we point the reader to other reviews in the field of NHCs [30–37].

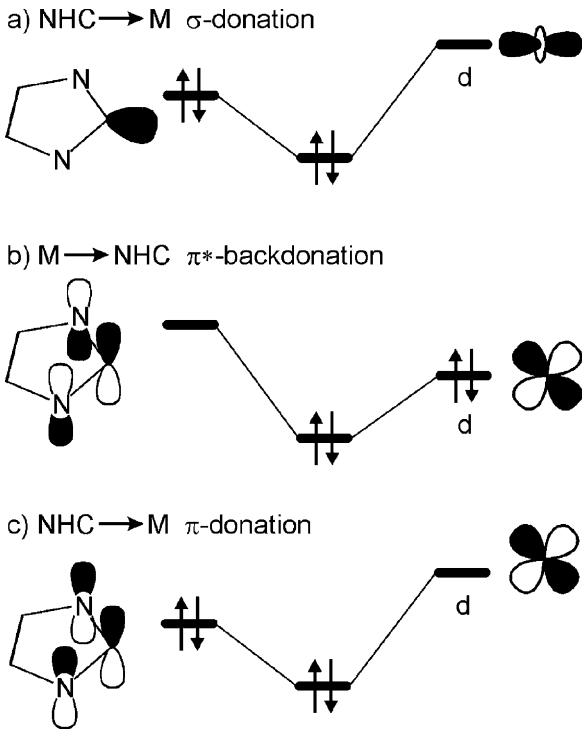

Fig. 1. The three bonding contributions to the M–(NHC) bond.

2. Electronic structure of NHCs and thermodynamics of dimerization

2.1. Electronic structure of NHCs

After the first synthesis of stable monomeric NHCs, spectroscopic studies immediately revealed their similarity with phosphines. Indeed, both these classes of ligands are σ-donor ligands with low π^*-backdonating character [38]. NHCs are neutral compounds with a divalent carbon atom with six electrons in its valence shell [34]. NHCs are bent carbenes, which means that the frontier orbitals are an sp^2-hybridized orbital and a p orbital orthogonal to the sp^2 plane, usually called σ and p_π, respectively. There are four possible electronic configurations for NHCs, see Fig. 2. NHCs are known to present a singlet $^1A_1$ ground state with a σ^2 configuration and discarding the high energy $^1A_1$ singlet state, with a $p_\pi{}^2$ configuration, the only competing electronic states are the triplet $^3B_1$ and the singlet $^1B_1$ electronic states that present single occupied σ and p_π orbitals. On this basis, it is clear that the stability of carbenes depends on the singlet–triplet σ-p_π gap, E_{S-T} [39]. If greater than 40 kcal/mol roughly, a singlet ground state is favored [40]. In the three classes of NHCs reported in Chart 1 the singlet–triplet gap is around 65–85 kcal/mol, which indicates clearly that the singlet $^1A_1$ electronic state with a σ^2 configuration is favored [39]. The main reason invoked to explain the stability of the singlet state is the inductive effect of the σ-withdrawing amine group substituents, which stabilizes the σ orbital on the carbene C atom. This stabilization of the σ orbital increases the singlet–triplet energy gap, and therefore the single state is favored [34]. Further stabilization is provided by p_π donation from the N atoms into the empty p_π orbital of the carbene C atom [34]. Further, it was suggested that a more bent bond angle at the carbene center should enhance stability of carbenes [41].

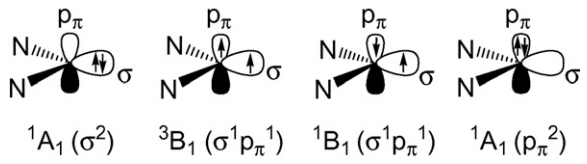

Fig. 2. Electronic configurations of NHC carbenes.

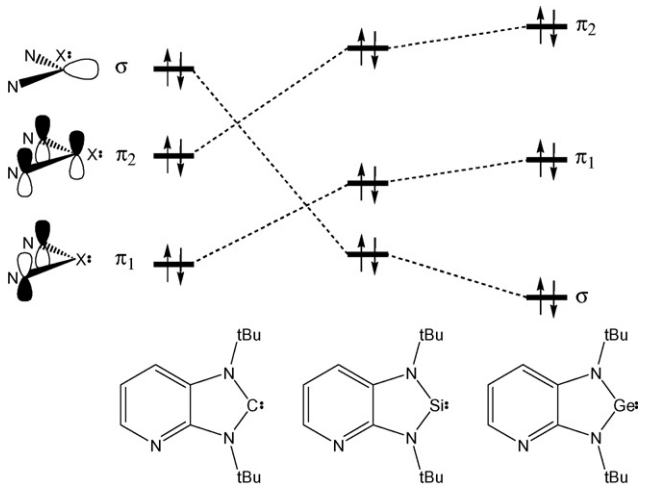

Fig. 3. Qualitative diagram of the frontier orbitals in annelated heterocyclic systems.

As a final note, we remark that in NHCs it is usually assumed that the HOMO corresponds to the σ lone-pair on the carbene C atom, with π molecular orbitals that include the p_π orbitals of the N atoms lower in energy. However, a recent combined experimental/theoretical study evidenced that in some cases [42,43], see, for example, the pyridoannelated systems of Fig. 3, an inversion in the stability of the σ and filled π molecular orbitals can occur for the higher silylene and germylene homologues [43].

The 5-membered ring of the basic skeleton of the NHC rings of Chart 1 is planar, although the N–CH_2–CH_2–N dihedral angle in the saturated imidazolin-2-ylidene NHCs deviates from a perfect eclipsed conformation by roughly 10°. For a long time, key questions addressed the aromaticity of the imidazol-2-ylidene NHC ring, as well as on the relevance of the resonance structures of Fig. 4. Independent reports by Apeloig and co-workers [44] and by Boehme and Frenking [45] cleared the issue. Based on fourth order Møller–Plesset theory methods, MP4, and coupled-clusters calculations with inclusion of single, double and perturbatively connected triple excitations, CCSD(T), Apeloig and co-workers explored several aromaticity criteria for the basic imidazol- and imidazolin-2-ylidene NHC rings, arriving at the conclusion that cyclic electron delocalization in imidazol-2-ylidenes is present to some extent, and that remarkable p_π donation from the N atoms to the carbene C atom occurs also in the imidazolin-2-ylidenes [44]. Similar conclusions were obtained by Boehme and Frenking, through the analysis of the electronic structure in the saturated and unsaturated NHC rings [44,45].

2.2. Thermodynamics of NHCs dimerization

In many cases NHC ligands have proven to be more effective than phosphines as ancillary ligands in catalysis [46,47], which started

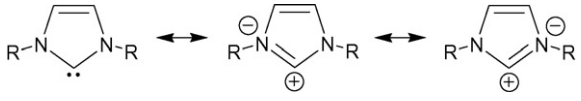

Fig. 4. Resonance structures for imidazol-2-ylidene NHCs.

an extensive search for new NHCs. Unfortunately, the search for new and useful NHCs remains extremely difficult, particularly for the saturated NHCs derived from the imidazolin-2-ylidene ring, because useful NHCs have to be synthesized as monomeric species, whereas monomeric NHCs have the disappointing tendency to easily dimerize as shown in Eq. (1), where $-E_{dim}$ is the energy gain associated with the dimerization of the two free NHC ligands.

$$2\text{NHC} : \rightleftharpoons \text{NHC}{=}\text{NHC} + -E_{dim} \quad (1)$$

Overall, the stability of monomeric NHCs depends on two aspects, steric and electronic. The electronic stabilization is related to the σ-withdrawing properties of the N atoms, but also depends on π-donation into the carbene p_π orbital from the π-system which involves the p_π orbital of the N atoms and can extend to the C4 and C5 atoms of the imidazol- and benzimidazol-2-ylidene rings [6]. On the other hand, steric effects due to bulky substituents on the N atoms protect the free NHC from dimerization. Of the three main families of NHCs shown in Chart 1, the family of unsaturated NHCs based on **3** revealed to be the one thermodynamically most stable towards dimerization [48–50].

Based on previous work by Carter and Goddard, that correlated the bond energy of alkenes to the singlet–triplet energy separation E_{S-T} of the corresponding carbenes [51], Heinemann and Thiel soon realized that the singlet–triplet energy separation is also the key to understand the relative stability of NHCs [39]. In particular, they calculated that E_{S-T} of saturated imidazolin-2-ylidenes, ~70 kcal/mol, is roughly 10 kcal/mol lower than that calculated for unsaturated imidazol-2-ylidenes, ~80 kcal/mol. The higher E_{S-T} of the unsaturated ring was correlated to its higher stability towards dimerization [39]. Similar analysis was performed by Cheng and Hu using the hybrid B3LYP functional [52], and they further evidenced that Cl substituents on the C4 and C5 atoms of the imidazol-2-ylidene skeleton reduces the E_{S-T} by roughly 5 kcal/mol relative to the unsubstituted ring, while Me substituents on the N atoms have a rather small influence [52]. In a following study, Cheng and Hu extended this approach also to NHC bearing bulkier N-substituents, such as *i*Pr groups, evidencing that *i*Pr groups slightly reduce the E_{S-T} with respect to Me substituents, but have a more sizeable effect on the dimerization energy, which was ascribed to the increased steric bulkiness of the *i*Pr substituents relative to Me substituents [53]. Almost at the same time, Nyulászi et al., in addition to the imidazol- and the imidazolin-2-ylidene rings, examined also a thiazol-2-ylidene carbene ring, in which one of the N atoms of the imidazol-2-ylidene is replaced by a S atom [54]. Using both a post-Hartree–Fock MP2 approach and a DFT B3LYP approach they found that the dimerization energy of the unsaturated thiazol ring is much closer to that of the saturated imidazolin ring, rather than to that of the unsaturated imidazol- ring. Further, they reported an excellent correlation between the dimerization energy of carbenes and the enthalpy of the isodesmic reaction of Scheme 1. Finally, they found that the B3LYP dimerization energies are systematically smaller than MP2 values.

The effect of the heteroatom in cyclic carbenes was investigated in details by Yates and co-workers [55]. They found that the *N*,*N* imidazol-2-ylidene carbene is thermodynamically the most stable towards dimerization, while progressive substitution of the N atoms with S, P and O leads to cyclic carbenes with much higher tendency towards dimerization. Further, in line with previous studies, they successfully correlated the dimerization energy of the various

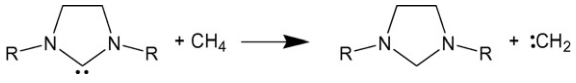

Scheme 1.

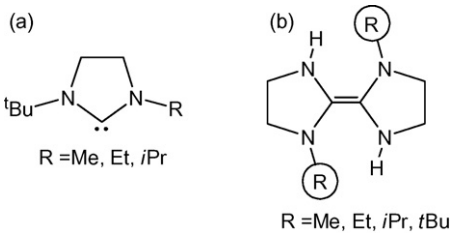

Chart 2.

carbenes with the enthalpy of the isodesmic reaction of Scheme 1, as well as with the singlet–triplet energy splitting E_{S-T}. However, they also warned that for carbenes with different steric requirements these empirical approaches to the dimerization energy could fail [55].

A comprehensive study was performed by Alder et al. Using a B3LYP DFT approach they examined a series of cyclic NHC of variable size (5-, 6- and 7-membered rings) with different alkyl substitution on the N atoms [32]. They clearly evidenced that increasing the bulkiness of the alkyl group (Me, Et, *i*Pr and *t*Bu) increases the stability of the monomeric NHC, and that this effects is less relevant for the 5-membered NHC since the N-substituents are pulled away from the carbene center due to the small N–C–N angle. Comparison of the Me substituted 5-, 6- and 7-membered NHCs indicated that the energies of dimerization of the 5- and 6-membered rings are rather similar, that dimerization of the 7-membered ring is favored by roughly 20 kcal/mol with respect to that of the smaller rings, and that it is quite close to the dimerization energy of the acyclic tetramethyl substituted diaminocarbene. This was somewhat surprising, since the 6-membered ring is apparently more similar to the 7 rather than to the 5-membered NHC [32].

Starting from the observation that none of the carbenes of Chart 2 dimerizes, Denk et al. recently reported on a systematic study on the thermodynamics stability of a series of symmetric and unsymmetric NHC ligands [56]. Calculations at the DFT B98/6-31G(d) level were performed on the NHCs of Chart 2a, as well as on model NHC systems in which the *t*Bu group is replaced with a H atom. The presence of only one sterically demanding alkyl substitutent allows to obtain enetetramines with substantially no steric pressure, see Chart 2b, allowing the separation between steric and electronic effects. This approach indicated that there is a regular increase of stability of the monomeric NHC for R = Me, Et, *i*Pr, *t*Bu, due to the increased electron donating properties of higher alkyls. Of course, the *t*Bu group stabilizes the monomeric NHC also for steric reasons. Further, comparison of the calculated ^{13}C NMR shift of the carbenes, and of the stretching frequency of the C=C double bond in the enetetramines, suggested that the variation in the dimerization energy on moving to higher alkyl substituents is mainly due to a progressive destabilization of the enetetramine rather than to a stabilization of the monomeric NHCs [56].

In summary, several studies have clearly evidenced that the dimerization tendency of a given NHC can be connected to its steric and electronic properties [32,39,51–55], and some attempts have been tried to propose empirical recipes to rationalize the dimerization energy of NHCs [54,55], or to separate steric and electronic effects cleanly [56]. Recently, an empirical recipe described by Cavallo and co-workers has rationalized the dimerization behavior of NHCs, and could be used to predict if a newly designed NHC will dimerize or not [57]. One of the limits is that this kind of calculations predicts only the thermodynamic stability of a given NHC, and says nothing on its possible kinetic stability.

In this approach the dimerization energy of a given NHC, $-E_{dim}$, is described by Eq. (2), where NHC_{Steric} and $NHC_{Electronic}$ are the

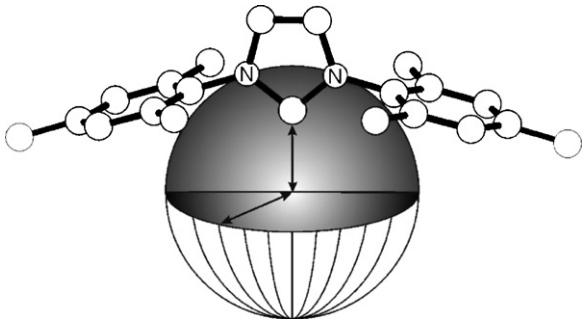

Fig. 5. Schematic representation of the sphere used for determination of the steric parameter $\%V_{Bur}$.

molecular descriptors able to capture the steric and electronic properties of a given NHC, respectively, while *A*, *B* and *C* are the empirical parameters fitted to reproduce a set of E_{dim} values.

$$E_{dim} = A \times \mathrm{NHC}_{Steric} + B \times \mathrm{NHC}_{Electronic} + C \quad (2)$$

Based on previous studies that clearly evidenced a correlation between the singlet–triplet energy gap and the dimerization energy, it was natural to set $\mathrm{NHC}_{Electronic} = E_{S-T}$. For the steric part, instead, it was assumed that $\mathrm{NHC}_{Steric} = \%V_{Bur}$, where $\%V_{Bur}$ is the buried volume, see Fig. 5, which is a molecular descriptor that can be considered as an analogue of Tolman's cone angle for tertiary phosphines [58]. The $\%V_{Bur}$ was successfully used to classify the steric properties of NHC ligands [33], see Section 3.7 for further details. Due to the paucity of experimental data [59], the E_{dim} that were fitted are DFT BP86 dimerization energies, E_{dim}^{DFT}. The E_{S-T} values and the geometries used for the calculation of the $\%V_{Bur}$ were also obtained from DFT calculations.

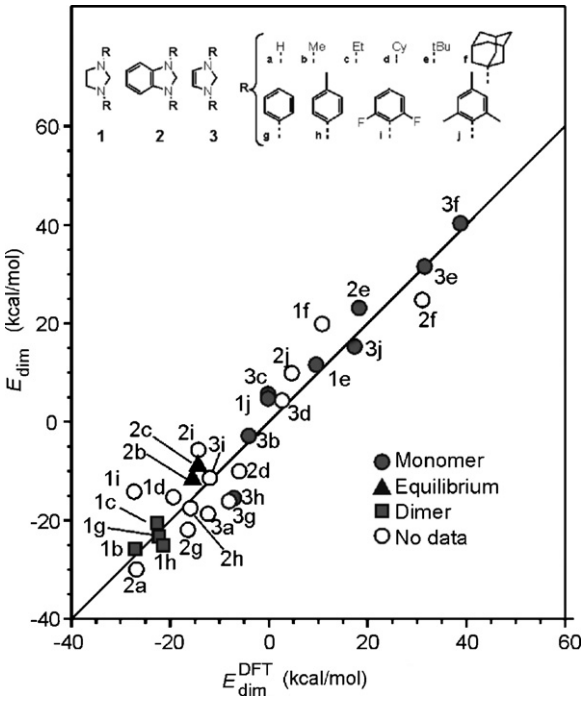

Fig. 6. Plot of E_{dim} vs. E_{dim}^{DFT} for the NHCs in the inset. The diagonal line is plotted to guide the eye. Black circles refer to NHCs that are known to be stable as free monomers, black triangles refer to NHCs that show a monomer–dimer equilibrium in solution, black squares refer to NHCs that are isolated as stable dimers, while empty circles refer to NHCs for which no experimental data is available.

Using this approach all the NHCs reported in the inset of Fig. 6 were considered. Optimization of the *A*, *B* and *C* parameters of Eq. (2) resulted in a very good correlation between the predicted dimerization energies, E_{dim}, and the dimerization energies obtained through DFT calculations, E_{dim}^{DFT}, see Fig. 6.

Considering that NHCs **3b** [60] and **1c** [61] of Fig. 6 are known to be stable as monomers and dimers, respectively, it was suggested an energy window separating NHCs that will be stable as monomers ($E_{dim}^{Fit} > -3$ kcal/mol) and NHCs that will dimerize ($E_{dim}^{Fit} > -22$ kcal/mol) [57].

3. The M—(NHC) bond

3.1. Performance of DFT methods to reproduce experimental values

Before entering into the discussion of the M—(NHC) bond, we give an overview of the performances of standard DFT approaches in reproducing a series of experimental results that involve complexes of NHCs with transition metals.

Although it is well accepted now that DFT methods are extremely effective in reproducing the X-ray geometries of transition metal complexes [62], it is worth to stress this point once more. A series of experimental and DFT M—(NHC) bond distances are reported in Table 1.

The DFT optimized structures reproduce the X-ray M—(NHC) distances with a rmsd of only 0.016 Å. Further, even small differences, such as the shorter Ru—(NHC) distance found for unsaturated NHCs with respect to the analogous saturated NHC, compare entries **2** and **3** in Table 1. However, it is important to stress that almost all these calculations have been performed with inclusion of relativistic effects with the zero-order regular expression (ZORA) [67–69] or with relativistic effective core potentials, since relativistic effects are relevant for accurate calculations on second and particularly third row metals.

Similar good agreement is obtained if the energetic of the M—(NHC) bond is considered. As shown in Table 2, the DFT bond dissociation energies of the NHC ligands, BDE, reproduce with good accuracy the relative calorimetric bond disruption enthalpies. First, there is a reasonable agreement between the absolute exper-

Table 1
Comparison between M—(NHC) bond distances from X-ray structures and DFT calculations

	Complex	M–(NHC), X-ray	M–(NHC), DFT	Reference
1	$Cp^*Ru(ITol)Cl$	2.068	2.044	[63]
2	$Cp^*Ru(IMes)Cl$	2.105	2.086	[63]
3	$Cp^*Ru(SIMes)Cl$	2.083	2.076	[63]
4	$Cp^*Ru(IPr)Cl$	2.086	2.093	[63]
5	$Cp^*Ru(SIPr)Cl$	2.087	2.078	[63]
6	$(TIME^{Me})_2Cu_3$[a]	1.912	1.901	[64]
7	$(TIME^{Me})_2Ag_3$[a]	2.082	2.087	[64]
8	$(TIME^{Me})_2Au_3$[a]	2.028	2.054	[64]
9	$(IMes)Ni(CO)_3$	1.971	2.005	[65]
10	$(SIMes)Ni(CO)_3$	1.960	1.969	[65]
11	$(IPr)Ni(CO)_3$	1.979	1.967	[65]
12	$(SIPr)Ni(CO)_3$	1.962	1.967	[65]
13	$(ItBu)Ni(CO)_2$	1.957	1.964	[65]
14	$(IAd)Ni(CO)_2$	1.953	1.964	[65]
15	$(IMes)Ir(CO)_2Cl$	2.108	2.099	[66]
16	$(SIMes)Ir(CO)_2Cl$	2.121	2.103	[66]
17	$(IPr)Ir(CO)_2Cl$	2.079	2.096	[66]
18	$(SIPr)Ir(CO)_2Cl$	2.071	2.098	[66]
19	$(ItBu)Ir(CO)_2Cl$	2.114	2.121	[66]

All distances in Å.

[a] $TIME^{Me}$ = Tripodal 1,1,1-tris[(3-methylimidazol-2-ylidene)-methyl]ethane carbene ligand.

Table 2
Relative experimental bond disruption enthalpies and DFT bond dissociation energies for a series of M—(NHC) bonds

	Complex	Relative BDE, experimental	Relative BDE, DFT	Reference
1	$Cp^*Ru(ITol)Cl$	18.8	26.2	[63]
2	$Cp^*Ru(IMes)Cl$	15.6	19.2	[63]
3	$Cp^*Ru(SIMes)Cl$	16.8	19.2	[63]
4	$Cp^*Ru(IPr)Cl$	11.1	11.6	[63]
5	$Cp^*Ru(SIPr)Cl$	12.1	10.9	[63]
6	$(ItBu)Ni(CO)_2$	39 ± 3	44.3	[65]
7	$(IAd)Ni(CO)_2$	43 ± 3	46.5	[65]

All BDEs are in kcal/mol.

imental values and the DFT values, although the DFT values are obtained from gas-phase calculations. Of course, this agreement is the consequence of compensation between various effects, such as reduced basis sets, basis set superposition errors, and neglect of solvent effects. Nevertheless, the calculated DFT BDEs reproduce the experimental trend that in the BDE of the $Cp^*Ru(NHC)Cl$ complexes, ITol > IMes ~ SIMes > IPr ~ SIPr [63], and that the BDE of ItBu in $(ItBu)Ni(CO)_2$ is smaller than that of IAd in $(IAd)Ni(CO)_2$ [65].

Since the M—(NHC) bond length and energy is reproduced with reasonable accuracy, it is reasonable that also vibrational properties are reproduced well by DFT methods. In Table 3 a comparison between the experimental and theoretical frequency of CO stretching in a series of Ir complexes is reported. The DFT values reproduce with very good accuracy (roughly $20\,cm^{-1}$) both the asymmetric (ν_{CO} ~$2000\,cm^{-1}$) and the symmetric (ν_{CO} ~$2070\,cm^{-1}$) CO stretchings. Within a given family of N-substituents (alkyl or aromatic) the DFT values replicate well the experimental trends. Furthermore, the DFT values can be also used to capture small differences between saturated NHCs (SIPr and SIMes) with their unsaturated counterparts. Indeed, the DFT values reproduce the experimental finding that both CO stretchings are about 1 or $2\,cm^{-1}$ smaller in the unsaturated NHCs. This finding suggested that in the saturated NHC-containing complexes there is a higher Ir → (NHC) π^*-backdonation, which consequently results in reduced Ir → CO π^*-backdonation. Before concluding, we warn that the calculation of vibrational properties on rather large complexes, such as those of Table 3, is extremely complicated because of the large number of different geometries these systems can adopt, which are very in close in energy.

A good agreement between the experimental and the theoretical data was obtained also in the calculation of the relative ^{195}Pt NMR chemical shift, σ_{Pt}, and Pt–C(NHC) spin–spin coupling constant, J_{Pt-C}, in the $(NHC)Pt(dmso)Cl_2$ (NHC = IMes, SIMes) complexes [70]. The DFT values correctly reproduced the experimental finding that the chemical shift σ_{Pt} of the Pt center in the IMes-based complex is moved downfield relative to that in the SIMes complex by roughly 20 ppm, and that the Pt–C spin–spin coupling constant J_{Pt-C} in the SIMes-based complex is smaller than in the IMes-based complex by roughly 120 Hz [70].

Table 3
Experimental and DFT-calculated carbonyl stretching of a series of $(NHC)Ir(CO)_2Cl$ complexes from ref. [66]

	Complex	ν_{CO} (cm^{-1}), experimental	ν_{CO} (cm^{-1}), DFT
1	$(ItBu)Ir(CO)_2Cl$	2065, 1980	2085, 2012
2	$(IAd)Ir(CO)_2Cl$	2063, 1980	2082, 2010
3	$(ICy)Ir(CO)_2Cl$	2065, 1981	2083, 2015
4	$(IMes)Ir(CO)_2Cl$	2066, 1980	2084, 2007
5	$(SIMes)Ir(CO)_2Cl$	2068, 1982	2085, 2008
6	$(IPr)Ir(CO)_2Cl$	2067, 1981	2083, 2005
7	$(SIPr)Ir(CO)_2Cl$	2068, 1982	2084, 2007

Finally, we remark that Green et al. compared the experimental photoelectron spectra of (NHC)–M–(NHC) (M = Pd, Pt) complexes with the ionization energies calculated at the BP86 DFT level. An overall good agreement between the pattern of calculated and experimental ionization energies was found [71].

3.2. NHC as σ-donors: the M–(NHC) σ-bond

In contrast with the classical carbene ligands, NHCs do not require π^*-backdonation from the metal into p_π orbitals of the carbene carbon atom in order to form stable adducts. Indeed, the stability of NHC-bearing complexes of main group elements and rare earth metals has been long used as an empirical evidence of their pure σ-donor character. A number of stable NHC adducts of main group elements [72–78], of alkali [79] and earth-alkali metals [80–82], as well as of ytterbium and samarium complexes [83–86] have been reported.

Within group 2 elements, beryllium is of particular interest due to the strong Lewis acidity of this cation. Since the first-report of a stable Be–(NHC) derivative by Herrmann et al. [87], a new field in carbene chemistry was opened. They showed that nucleophilic carbenes as IMe can split the polymeric structure of beryllium dichloride to form tris-carbenic ionic complexes of general formula $[(Cl)Be(IMe)_3]^+[Cl]^-$. The bonding situation in Be–(NHC) derivatives was investigated by Frenking and co-workers using *ab initio* calculations at the MP2 level of theory on beryllium-carbene model systems of general formula $Be(CX_2)_n^{2+}$ (X = H, F; n = 1–4), $ClBe(CX_2)_n^+$ (X = H, F; n = 1–3), and $Cl_2Be(CX_2)_n$ (X = H, F; n = 1, 2) [88]. Natural bond orbital analysis supported the idea that the carbene ligands are pure σ-donors in these complexes. The dications $Be(CX_2)_n^{2+}$ have strong Be^{2+}—C donor–acceptor bonds. The $:CH_2$ complexes have stronger Be—C bonds than the $:CF_2$ complexes, but the $:CH_2$ complexes were predicted to be less stable than the $:CF_2$ complexes for kinetic reasons. The carbon p_π orbital of the methylene moiety stays nearly empty in the $Be(CH_2)_n^{2+}$ complexes, which makes them prone to nucleophilic attack. In the $Be(CF_2)_n^{2+}$ complexes the p_π donation from the fluorine atoms stabilizes electronically the complexes. These results clearly supported the idea that the key factor in the isolation of stable carbene complexes is the population of the p_π orbital of the carbene C atom, which can be increased by π donation from the atoms bonded to the carbene C atom. Since no back-donation is possible in the case of beryllium, π-donation from the substituents of the carbene C atom (the N atoms in NHCs) improving coordination to a pure acceptor metal, can explain the stability of the complex obtained by Herrmann. Focusing on the heavier members of group 2, the first stable adducts of alkaline earth metals with NHC ligands were reported by Arduengo et al. in 1998 [81]. In this structural study a series of 1,3,4,5-tetramethylimidazol-2-ylidene adducts with $(Cp_5Me_5)_2M$ ($Cp = \eta^5$-cyclopentadienyl, M = Mg, Ca, Sr, Ba) was compared. The nature of the M—(NHC) bond showed smooth trends, with M—C bonds ranging from somewhat covalent for magnesium to rather ionic for barium, with a dependency of the metal–carbene bond strength on the size of the alkaline earth metal. A number of different adducts of IPr with complexes of Mg, Ca, Sr and Ba with substituted Cp were carefully studied by NMR and crystallography techniques by Schumann et al. [82]. They showed that the imidazol-2-ylidene ligand prefers to bind the alkaline earth center by σ-donation. However, examination of the M–C(NHC) distances in these complexes (Mg–C(NHC) < Ca–C(NHC) < Ba–C(NHC)) indicates that the stronger σ-interactions are observed with the lighter alkaline earth metals. This trend is also supported by the ^{13}C NMR chemical shift of the carbene center coordinated to the various metals.

Erker and co-workers reported the synthesis and the bonding analysis of carbene adducts of the cationic group 4 metallocene

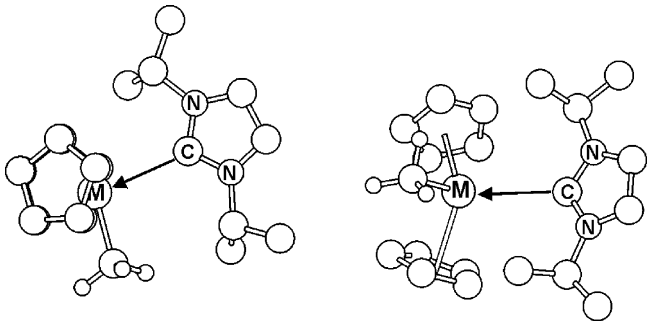

Fig. 7. Schematization of the favored "*in plane*" conformation (left-side) and of the less stable "perpendicular" conformation (right side) of cationic $[Cp_2TiCH_3(NHC)]^+$ complexes.

complexes such as those of Fig. 7 [89]. They found that the structural characteristic feature of these complexes is the conformational arrangement of the NHC ligand with respect to group 4 bent metallocene framework. X-ray crystal data showed that the NHC ligand was bonded to the transition metal in an orientation where the NHC ring lies in the equatorial belt of the metallocene moiety. NMR analysis indicated the absence of a rapid rotation around the M—(NHC) bond for both metallocenes. Theoretical investigation at the DFT level of the complexes of Fig. 7 and of a series of related models revealed that the observed "*in plane*" orientation of the NHC ligand is steric in nature. It takes origin in the steric repulsion between the bulky isopropyl substituents of the NHC ligand and the Cp ligand, see Fig. 7. The bonding between the imidazol-2-yldene ring and the cationic $Cp_2TiCH_3^+$ moiety was analysed considering a fragment approach within an overall C_S symmetry. Frontier orbital analysis displayed that the overall bonding situation of the NHC ligand does not match with the one observed for Fischer type carbene complexes. The bonding interaction between the HOMO of the NHC, mainly composed of the donating lone pair of the NHC, and the two lowest lying empty orbitals of the metallocene fragment leads to a low-lying metal–(NHC) σ-bond. Charge distribution analysis of the complexes indicated no remarkable differences between the "*in plane*" conformation (global minimum) and the less favoured "perpendicular" conformation (see Fig. 7). The absence of a dependence in the charge distribution upon the NHC rotation confirmed the main σ-orbital character of the M—(NHC) bond and the lack of π-contributions. This study was extended through the DFT analysis of a series of bis-Arduengo carbene complexes of group 4 metal halide of the type $MCl_4(NHC)_2$ [90,91]. Bonding analysis supported again the idea that the NHC ligands serve as pure σ-donor in these cases.

Still on group 4 M–(NHC) systems, DFT Ti–(NHC) bond energies calculated by Roesky and co-workers in complexes of general formula L–$[TiF_5]^-$ (L = IMe, F^-, Cl^-) resulted in the following order of the relative basicities: $Cl^- < IMe < F^-$, in agreement with the experimental order extracted from the NMR data [92].

Over the years, several theoretical studies supporting the idea that the M–(NHC) bond is mainly a σ-bond in nature were reported also for late transition metals. Lee and Hu reported on a systematic DFT analysis of a number of different NHC ligands in $Cr(CO)_5L$ complexes, L being different imidazol-2-ylidene or imidazolin-2-ylidene based NHC ligands, as well as acyclic carbenes, and phosphines by Lee and Hu [93]. NHCs ligands showed Cr–C distances longer than those observed for other carbenes. Comparison of the NHC dissociation energies and of the Cr–(NHC) distances in imidazol-2-ylidene and imidazolin-2-ylidene complexes suggested that π-delocalization in the ring of the NHCs does not affect the nature of the M—(NHC) bond, since both parameters are scarcely dependent on the nature of the NHC ring. Further analysis indicated that for these NHCs complexes π-backdonation is negligible compared to the σ-donation.

Group 10 metals (Ni, Pd, Pt) bis(carbenes) complexes are a prototypical example of stable neutral two-coordinated complexes. As for the isoelectronic complexes of group 11 metal ions (Cu^+, Ag^+, Au^+), they show a linear coordination at the metal atom [94], which is common for d^{10} metals. The crystal structure of the $M(ItBu)_2$ (M = Pd, Pt) complexes presents an approximate D_{2d} symmetry with the two rings orthogonal to each other. The M—(NHC) bond in these systems has been investigated by Green et al. [71] by a combination of photoelectron spectroscopy and DFT BP86 calculations. Molecular orbitals analysis indicated that the primary bonding orbital, σ_g, is a linear combination of the carbene lone pairs and of a metal (d_{z2} + s) hybrid. The photoelectron spectrum of the $Pd(ItBu)_2$ and $Pt(ItBu)_2$ complexes were compared with that of the free ligand, and the change in the band profile after complexation was found to be consistent with the stabilization of the σ_g linear combination of the lone pair in the complex. DFT calculations were performed on the model systems M(imidazol-2-ylidene)$_2$ under the assumption of a perfect D_{2d} symmetry. Ionization energies were calculated both by the Slater's transition state method [95] as well as by calculating the cationic $[M(NHC)_2]^+$ species in the ion ground state and the first eight excited states using the optimized geometries of the molecules. The agreement between the pattern of calculated and experimental ionization energies confirmed that in these systems the main bonding occurs through σ donation from the NHC lone pair into the metal hybrid (d_{z2} + s) orbital, and suggested an almost negligible π contribution to the M—(NHC) bond [71].

More recently, Penka et al. expanded the theoretical understanding of NHC bonding to group 10 electron rich metal complexes [96]. They analyzed, at the DFT PW91 level with inclusion of relativistic corrections by the ZORA method [67–69], the M—(NHC) bond in complexes of general formula $[MX_3(imidazol\text{-}2\text{-}ylidene)]^-$ (X = H, Cl, I and M = Ni, Pd, Pt). The bonding scenario in these complexes was compared with that calculated for the corresponding pyridine complexes $[MX_3(Py)]^-$. The main result was that the σ-character in the M—(NHC) bonds is considerably stronger than in the M—(Py) bonds. Although in the NHCs complexes the π-acceptor interactions generally increases from I < Cl < H, as consequence of the higher charge density on the metal in the MX_3^- fragment, the ratio between σ and π contributions to the M–(ligand) bond are calculated to be higher for NHCs complexes indicating the dominant σ-donor nature of metal–(NHC) bond in the analyzed complexes [96]. Further on group 10 complexes, Ghosh and co-workers investigated $(NHC)PdX_2(pyridine)$ (X = Cl, Br) complexes, and based on a charge decomposition analysis they concluded that NHC are strong σ donors with minimal π^* accepting capability with rather high σ/π^* ratios [97].

NHC complexes of group 11 cations were theoretically investigated by Boehme and Frenking [98]. They reported post-Hartree–Fock calculations at the MP2 level of theory for the complexes of CuCl, AgCl and AuCl with the imidazol-2-ylidene NHC ligand and the related silylene and germylene ligands. The calculated metal–ligand dissociation energies, D_e, indicated that these NCH complexes have very strong M–(carbene) bonds. In particular, the (NHC)—AgCl bond (D_e = 82.8 kcal/mol) was calculated to be even stronger than the W—(CH(OH)) bond (D_e = 75.0 kcal/mol) in the classical $(CO)_5W(CH(OH))$ Fischer carbene complex, whose strength is increased by a relevant π^*-backdonation interaction [99]. Within the group, the D_e trend was calculated to be Au > Cu > Ag, for all the ligands (carbene, silylene and germylene) considered. As for a ligand effect (carbene, silylene, and germylene), the D_e trend was calculated to be C > Si > Ge. The M–(ligand) donor–acceptor interactions were investigated by charge decomposition analysis [100]. The orbital contributions were divided into

three parts: (1) L → MCl σ-donation from the ligand to the metal; (2) MCl → L π^*-backdonationfrom the MCl fragment to the ligand; and (3) repulsive polarization between the L and MCl fragments, due to the mixing of occupied orbitals of L and MCl. The main result was that the σ-donation was found to be always remarkably larger than the π^*-backdonation [98], and the σ/π^* ratios were calculated to be significantly larger than that calculated for classical Fischer carbene compounds. The influence of the π^*-backdonation was found to be a bit stronger in silylene and germylene with respect to the carbene complexes, where it was found to be substantially negligible, which suggested that σ-donation is the dominant term of the M—(NHC) bond. The covalent contribution to the L—MCl bond arises from donation of the σ-lone pair of the ligand to a metal (d_{z2} + s) hybridized orbital. Although a significant covalent contribution was also calculated, topological analysis of the electron density distribution in the complexes suggested that the M—(NHC) bond has a strong ionic character which comes from electrostatic interaction between the positively charged metal atom and the σ-lone pair of the donor atom of the ligand. The charge decomposition analysis mainly confirmed the almost pure σ-donor character of the carbene ligands. Comparison between complexes and free ligands showed that the p_π population of the ligand donor atom X (X = C, Si, Ge) is slightly higher in the complexes. However, it was suggested that this extra p_π charge is not due to π^*-backdonation but to a slightly enhanced aromaticity of the ligands in the metal complexes. In fact, the N–X bond order was found higher in the complexes than in the free ligands, indicating a rather stronger N–X π-donation [98]. It is noteworthy that a somewhat higher π^*-backdonating contribution has been calculated for AuCl–carbene complexes, which was ascribed to relativistic effects that lead to a contraction of the s and p orbitals but to more diffuse d and f orbitals. Relativistic effects have been recognized to be very important in the description of gold compounds [101–104].

DFT studies of NHC complexes with coinage metals have been performed by Ghosh and co-workers, and they found that in the (NHC)–M–(NHC) systems the NHC is an almost pure σ donor [105]. They also investigated the neutral dimeric Ag and Au complexes of Chart 3a. The Ag–Ag interaction was found to be stronger than the Au–Au interaction. Analysis of M–(NHC) interaction indicated that the NHCs are effective σ-donors with relatively weaker π^*-accepting character [106]. Further, they investigated the macrometallacycle complexes of Chart 3b, and evidenced that in these cyclic systems the main NHC donation involves empty s orbital of the metal (5s for Ag and 6s for Au), whereas in the corresponding monomeric species donation occurs primarily at an empty p orbital of the metal [107].

Finally, still on group 11 metals, it is worth mentioning a DFT study focused on the mechanism of formation of the very popular complexes of the type (NHC)Ag–X (X = halide) performed by Peris and co-workers [108].

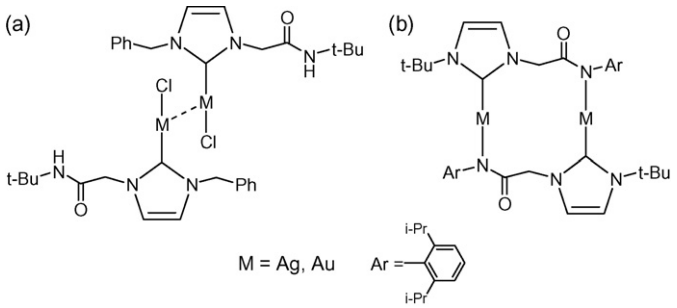

Chart 3.

Particular efforts have been devoted to study the difference, in bonding properties, between saturated and unsaturated NHCs. Nolan and co-workers reported a combined experimental and theoretical study examining the bonding properties of NHCs in the [(Cp^*)Ru(NHC)Cl] system comparing saturated ligands, such as SIMes and SIPr, with their unsaturated analogues IMe and IPr [63]. Computational and structural investigations showed that the M—(NHC) bond distances are systematically slightly shorter for saturated NHC with respect to their unsaturated analogues. This finding, in conjunction with calorimetric and DFT BP86 studies of the M—(NHC) bond strength involving saturated and unsaturated NHC complexes, suggested that saturated NHC are slightly better donor ligands, by roughly 1 kcal/mol, with respect to their unsaturated analogous. More recently, the same authors reported the synthesis and detailed spectroscopic and computational analysis of [(NHC)Pt^{II}] compounds [70]. NMR results and electron density analysis confirmed the stronger σ-donor ability of saturated NHC with respect to the unsaturated ones. A similar preference for the binding of saturated versus unsaturated NHC was calculated by Caulton and co-workers. Based on B3PW91 DFT calculations they found that SIMe binds more strongly than IMe to $RuHCl(PH_3)_2$ moiety [109].

3.3. NHC as π-acceptors: the π^*-backdonation contribution to the M–(NHC) π-bond

For almost a decade, NHC ligands were considered to be pure σ-donors with substantially insignificant π^*-backdonation capability. However, a few seminal reports [110–112], particularly that by Meyer and co-workers [112], evidenced that NHCs have π^*-backdonation capability, and this contribution in some cases is not negligible.

3.3.1. NHC–non-metals (C, N, O, Si, P, S) systems

B3LYP/6-31G* calculations were carried on (NHC)–carbenoid adducts were the NHC is imidazol-2-ylidene and the carbenoid fragments are CH_2, NH, O, SiH_2, PH, and S, see Chart 4.

According to these studies, the bonding between the NHC and the CH_2, SiH_2, PH, and S carbenoid moieties is best described as a donor–acceptor bond, consisting not only of σ donation from the NHC but also from π^*-backdonation of the carbenoid fragment into π^* orbitals of the NHC group. However, when dealing with the NH and O fragments, the electronegativity of the heteroatoms results in a mainly σ-bond [72].

3.3.2. NHC complexes with group 4 and 5 metals (Ti, Zr, Hf, V)

DFT studies performed on (IMe)–$Ti(NMe)_2Cl_2$ [113] and (IMe)–$V(O)Cl_3$ [114] pointed out that there is a substantial bonding overlap between the lone pair of the cis chloride ligands and the formally vacant π-orbital of the carbene carbon atom of the NHC ligand. This kind of interligand bonding interactions involves a significant contribution from the d orbital of the V and can be considered a sort of π-backdonation to the NHC with electron density transferred from the Cl lone pairs to the metal.

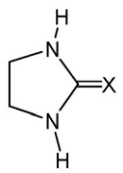

X = CH_2, NH, SiH_2, PH, S

Chart 4.

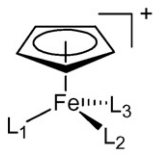

	L_1	L_2	L_3
1.	CO	CO	CO
2.	CO	CO	Py
3.	CO	CO	NHC
4.	CO	Py	Py
5.	CO	NHC	Py
6.	CO	NHC	NHC

Chart 5.

BP86 DFT calculations performed by Jacobsen et al. on d^0 metal complexes of V, Ti, Zr and Hf indicated that in these systems the M → NHC π^*-backdonation usually is around 10% of the total orbital interaction energy [115]. More details on this point can be found in Section 3.6. Similar DFT studies, at BP86/TZ2P level, recently conducted on (NHC)–MCl_4 complexes, with NHC = "normal" imidazol-2-ylidene and "abnormal" imidazol-4-ylidene ligands (see Chart 1) and M = Ti, Zr, Hf, indicated that the π contribution to the orbital interaction is about 12–13%, and half of it corresponds to a M → NHC π-backdonation. Nevertheless, the author pointed out that in these complexes the electrostatic interaction between the NHC ligand and the metal plays the main role in total bond energy [116]. Further, they also calculated stronger M—(NHC) bonds down the group 4 metals triad, which is in line with classical organometallic knowledge.

3.3.3. NHC complexes with group 6 metals (Cr, Mo, W)

A combined experimental and theoretical charge-density study on the (IMe)$Cr(CO)_5$ complex revealed a σ-donor/π-acceptor character of the NHC ligand [117]. This conclusion was suggested by the fact that the calculated bond distances in the 5-membered ring of the free NHC ligand are not significantly different after NHC complexation to the $Cr(CO)_5$ moiety. According to the authors, this is inconsistent with only a σ-donation M–(NHC) interaction, which should shorten the C—N bonds of the NHC ligand after complexation.

A more general bonding analysis of (NHC)$M(CO)_5$ complexes, with NHC = "normal" imidazol-2-ylidene and "abnormal" imidazol-4-ylidene ligands and M = Cr, Mo, W DFT studies, at BP86/TZ2P level, was reported by Frenking and co-workers [116]. According to this study, the considered d^6 metal systems present a π contribution to the total orbital interaction between the metal and the NHC about 17–18% of the total orbital interaction, and about 77–78% of the π orbital interaction has been attributed to the M → NHC π^*-backdonation. These results are in agreement with a previous DFT study by Jacobsen et al. [115], see Section 3.6 for more details.

3.3.4. NHC complexes with group 8 metals (Fe, Ru, Os)

Piano-stool Fe(II) complexes of the type [Fe(Cp)(CO)(NHC)(L)]X (L = pyridine, NHC, CO; X = I, BF4) were prepared by Albrecht and co-workers [118]. Electrochemical measurements allowed to determinate the Lever's parameters [119,120] of pyridine and NHC, which indicated similar donor properties for both ligands. Since σ donation of NHC ligands is well accepted to be stronger with respect to pyridines, the authors argued that also the M → NHC π^*-backdonation must be stronger in NHC than in pyridines bearing complexes, to balance the total charge transfer. DFT calculations at BP86/TZP level confirmed this hypothesis. Calculations were performed on the six simplified systems described in Chart 5 (Py = pyridine; NHC = imidazol-2-ylidene).

As for system **1**, **2** and **3** of Chart 5, energy decomposition analysis indicated that the M—(NHC) bond (ca. 80 kcal/mol) is stronger than the M–(pyridine) and M—(CO) bonds (ca. 50 kcal/mol), and that the π contribution to the total orbital interaction of the Fe—L bond is similar for pyridine and NHC (17.8 and 15.4% for **2** and **3**, respectively). In the presence of a larger σ donation, as for **5** and **6**, the π contribution increases up to 28%.

An experimental and computational study on $(P^iPr_3)_2Ru(Cl)(H)(NHC)$ complexes with NHC = IMe, SIMe and the 7-membered cyclic saturated NHC with Me substituents on the N atoms was conducted by Caulton and co-workers [109]. They compared the π-acidity of the unsaturated IMe and saturated SIMe NHC ligands. Based on the B3PW91 DFT calculations they found that the exchange reaction of these two ligand on the Ru fragment, is thermoneutral (bonding of the SIMe is favored by 1.1 kcal/mol only), suggesting that none of these cyclic carbenes is more effective in giving a stronger Ru—C bond. They concluded that both carbenes are primarily bound to the metal by a σ bond, because in case of a strong π interaction the aromaticity of the unsaturated IMe ligand should have stabilized the Ru fragment. Nevertheless, the small variations in the calculated bond lengths, together with the experimental bond lengths, in a very electron rich metal such as Ru in $Ru(H)(Cl)(PR_3)$, also suggested that π^*-backdonation in both carbenes is not negligible.

Some other NHC complexes of group 8 metals were investigated by a systematic bond analysis, using BP86 DFT methods [115], see Section 3.6 for further details. We anticipate here that the reported π contribution to the total orbital interaction is about 15–17% for all d^8 metal systems, whereas it drops to 10–11% for the d^6 metal systems. The π M—(NHC) bond is mainly due to π-backdonation, which can be over 80%. Similar conclusions were reported by Frenking and co-workers [116].

3.3.5. NHC complexes with group 9 metals (Co, Rh, Ir)

One of the most elegant experimental evidences of the relevance of π^*-backdonation was reported by Bielawski and co-workers [121]. They synthesized the (NHC)RhCl(cod) (cod = *cis*,*cis*-1,5-octadiene) complex sketched in Chart 6, where the 4, 5 positions of the NHC ring are fused with a *p*-quinone.

The exchange of the cod (with relatively little π^*-backdonating capability) with a CO (with relatively high π^*-backdonating capability), and the use of IR spectroscopy and cyclic voltammetry to observe structural and electronic changes in the corresponding complexes, revealed the presence of M → NHC π^*-backdonation in these complexes. In fact, the carbonyl stretching in the quinone increases when substituting the cod with CO, and the reduction potential of the complex presenting cod is greater than in the complex presenting CO. All data supported the hypothesis that, as a consequence of the π^*-backdonation, the NHC is more electron-rich in the (NHC)RhCl(cod) complex than in the (NHC)RhCl(CO) complex. More recent IR and NMR studies conducted by the same group on similar Rh complexes demonstrated that NHC ligands not only present π^*-acidic behaviour, but it is also possible to tune the amount of π^*-backdonation by changing the substituents (e.g. H, Cl, CN) in positions 4, 5 of the NHC ring [122].

The $Cp^*(NHC)Ir = Pmes^*$ complex, see Chart 7, was synthesized and characterized by X-ray diffraction by Lammertsma and co-workers [123]. Bond analysis through BP86 DFT calculations with inclusion of relativistic corrections through the ZORA method [67–69] on model complexes of general formula [Cp(NHC)Ir = E] (:E = :PH, :NH, $:CH_2$) showed that the NHC behaves as a strong σ

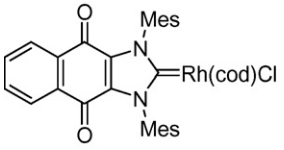

Chart 6.

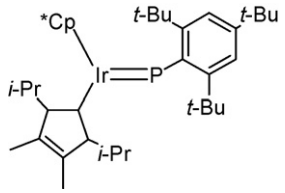

Chart 7.

donor and weak π-acceptor ligand and that the single M—(NHC) bond is very strong for :E = :PH and :CH_2, and much weaker for :E = :NH [123].

3.3.6. NHC complexes with group 10 metals (Ni, Pd, Pt)

In 1994 Arduengo reported on the first isolated 14 electron Ni(0) and Pt(0) complexes presenting 2 IMes NHC ligands. Structural X-ray diffraction studies revealed unusual short M—(NHC) bond distances that, according to the authors, would be rationalized only considering a contribution from M → NHC π*-backdonation.

PW91 DFT calculations with inclusion of relativistic corrections through the ZORA method [67–69] on square planar anionic d^8 complexes of general formula $[MX_3(\text{imidazol-2-ylidene})]^-$ (X = H, Cl, I and M = Ni, Pd, Pt), were conducted by Penka et al. [96]. The results were compared with analogous pyridine complexes $[MX_3(Py)]^-$. According to this study both the π-acceptor ability and the σ bonding of the NHC in these complexes are higher than in the corresponding pyridine complexes. Nevertheless, due to the strong σ contribution in the NHC complexes, the π/σ ratio results higher in the pyridine complexes, see also Section 3.2. The π-acceptor contribution increases in the order I ≤ Cl < H, due to the increase of the charge on the metal. Moreover, the π-bonding contribution increases in the order Pt < Pd < Ni.

The synthesis, structural characterization and BP86 DFT bond analysis of *cis*-[(IPr)Pt(dmso)$(Cl)_2$], *cis*-[(IMes)Pt(dmso)$(Cl)_2$], *cis*-[(SIPr)Pt(dmso)$(Cl)_2$], *cis*-[(SIMes)Pt(dmso)$(Cl)_2$], see Chart 8, was reported by Nolan and co-workers [70]. Unsaturated NHCs behaves as weaker ligands, being a less σ-donating and less efficient π*-acceptors. The π*-backdonation was estimated to contribute about 13% to the character of the bond. According to the authors, the catalytic activity of the systems would be affected by the nature of the NHC ligand because saturated NHCs bind more strongly to the metal, stabilize the catalytic system, but make the metal a worse σ acceptor and π donor for an incoming substrate. On the other hand unsaturated NHC ligands make the coordination of substrate more facile, but could give rise to stability issues, because of the weaker M—(NHC) bond.

Bond analysis DFT studies were performed by Jacobsen et al. [115] on d^{10} metal systems [(NHC)M$(\text{ethylene})_2$] (with NHC = imidazol-2-ylidene, and M = Ni, Pd, Pt) and [(NHC)Ni$(CO)_2$]. Both Ni(0) presented relatively high π contribution (24–25%) to the total bond orbital interaction, with more than 95% of it due to M → NHC π*-backdonation. Pd(0) and Pt(0), instead, present a π contribution smaller than 20%, 85–90% of which is due to the M → NHC π*-backdonation.

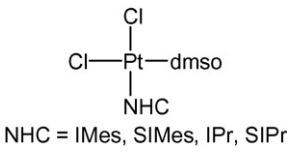

Chart 8.

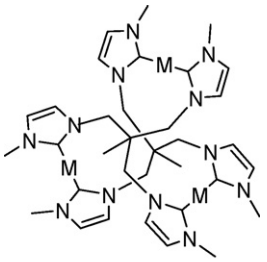

Chart 9.

3.3.7. NHC complexes with group 11 metals (Cu, Ag, Au)

In 2003 Meyer and co-workers reported on the synthesis and characterization of the NHC tridentate polycarbene silver complexes $[(TIME^{Me})_2Ag_3]_2(Ag_8Br_{14})$ and $[(TIME^{Me})_2Ag_3]_2(PF_6)_3$ ($TIME^{Me}$ = [1,1,1-tris(3-methylimidazolium-1-yl)methyl]ethane) [112], see Chart 9. The X-ray data indicated that the imidazol ring in the $[(TIME^{Me})_2Ag_3]_2(PF_6)_3$ complex presents elongated C–N bond distances, smaller N–C–N angles, and longer C=C bond distance with respect to the starting imidazolium salt $[TIME^{Me}](Br)_3$. This would be consistent with an increase of the π character of the carbene carbon and a decrease of the π delocalization on the imidazole rings.

BP86 DFT calculations with inclusion of relativistic effects (ZORA method) were conducted on the tricationc unit. Analysis of the frontier orbitals showed that the M—(NHC) bond mainly consists in a σ interaction involving the NHC lone pair and the silver hybrid d_{z2} + s, but a significant π bonding interaction between the NHC and the Ag metal atom, due to linear combination of the carbene p_π orbitals and the metal d_{xz}/d_{yz} orbitals, is also established. Furthermore, starting from the Ag complex $[(TIME^{Me})_2Ag_3]_2^{3+}(PF_6)^-_3$, the corresponding Cu and Au complexes were synthesized [64], see Chart 9, and DFT calculations were performed for all systems. Also in this case the bonding analysis revealed a non-negligible π M–(NHC) interaction. BP86 DFT calculations on simplified diaminocarbene complexes of all group 11 metals, showed that the π contribution in the M—(NHC) bond can be quantified as 15–30% of the overall orbital interaction energy [64].

NHC interactions with group 11 metals were also extensively studied by Frenking and co-workers by DFT calculations at BP86 level using an energy decomposition analysis [124]. The considered systems are depicted in Chart 10.

As for (NHC)–MCl systems, the (NHC)–M total interaction energy increases in the order Ag < Cu < Au, while focusing on the halide it increases in the order I < Br < Cl < F. More than 75% of the attractive energy is attributed to the electrostatic contribution. The π contribution to the total orbital energy falls in the range 27–38% and decreases in the order F > Cl > Br > I, for the silver systems, and as Ag < Cu < Au for the chloride systems. The energy decomposition analysis of the bis(carbene) complexes showed the same trend for the strength of the (NHC)—M bond (Au > Cu > Ag), and slightly more important orbital interactions than in the (NHC)–MX complexes.

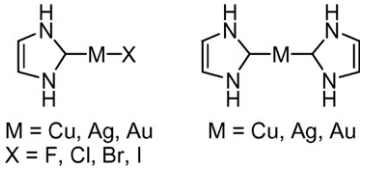

Chart 10.

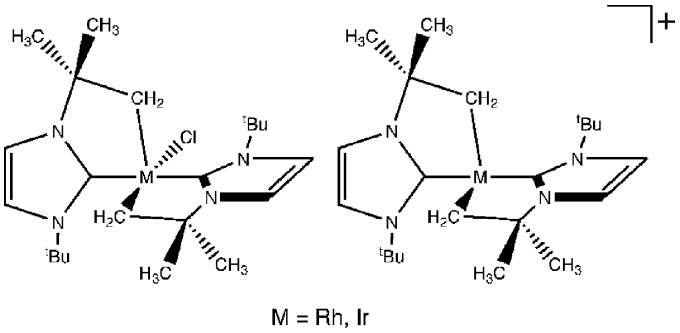

Chart 11.

3.4. NHC as π-donors: the π-donation contribution to the M–(NHC) π-bond

The π-donor capability of NHC ligands toward transition metals has been taken into account only in the past few years and seems to play an important role in electron poor complexes. The systematic bond analysis conducted by Jacobsen et al. [115] on d^0, d^4, d^6, d^8 and d^{10} metal complexes (see Section 3.6 for details) showed a trend in the π contribution on moving from electron-poor to electron-rich systems. Indeed, even if the π contribution to the total orbital interaction energy (σ + π) gradually increases on going from d^0 to d^{10} metals, the percentage of NHC → M π-donation with respect to the overall π contribution decreases. Similar results were obtained by Frenking and co-workers which performed a bond analysis on different d^0, d^6, d^8 and d^{10} systems [116]. The NHC → M π-donation was shown to follow the same trend, with a decrease from 48% in (NHC)$TiCl_4$ to 9% in (NHC)CuCl. Moreover, moving down the triad in analogous complexes the NHC → M π-donation generally decreases for heavier metals, with the exception of group 11 metals.

The significant role of NHC → M π-donation was well established in Rh and Ir electron poor 16 and 14-electron complexes, synthesized by Nolan and co-workers [125,126]. BP86 DFT calculations with inclusion of relativistic effects (ZORA method), were conducted on the 16e metal $MCl(ItBu')_2$ and 14e metal $[M(ItBu')_2]^+$ (M = Rh, Ir) complexes shown in Chart 11.

Natural bond order (NBO) analysis indicates that the neutral complex (which does not present equivalent NHC—M bond lengths, as shown both by DFT study and X-ray diffraction) present a higher bond order for one of the two NHC—M bond mainly due to a partial π-d donation from the filled π MO highest in energy of the NHC ligand to the empty d MOs of the metal. The cationic complex is characterized by a local C_2 symmetric axis and the HOMO-3 and HOMO-4 orbitals show a strong interaction between the filled π MO highest in energy of the NHC ligand to the empty d MOs of the metal. These results, together with further studies conducted on simplified model, indicate that the ability of NHC ligands to act as a π donor represent a key in understanding the remarkable stability of electron poor complexes.

3.5. Energy decomposition analysis of the M—(NHC) bond

Since energy is the crucial factor for structure and reactivity of chemical entities, energy decomposition analyses are most helpful for gaining information about the driving force leading to molecular geometry and reactivity. Energy decomposition schemes allow for a quantitative description of qualitative bonding concepts such as σ- and π-bonding, as well as donation and backdonation. Other partitioning schemes that are often employed in characterizing the nature of a chemical bond are based on charge analysis [127], or make use of a charge decomposition scheme [100]. A multitude of complexes of N-heterocyclic carbenes with transition metal centers M–(NHC) has been subjected to a partition analysis [37,64,93,98,103,112,115–117,124,128–131], which has provided valuable insights into the nature of the M—(NHC) bond. Most studies explore "normal" NHC ligands derived from imidazol-2-ylidene. A recent work extends the list of NHC tautomers to include "abnormal" NHC ligands derived from imidazol-4-ylidene as well as imidazole itself [116], while another study focused on pentacarbonyl Cr-Fischer complexes with acyclic carbenes [132].

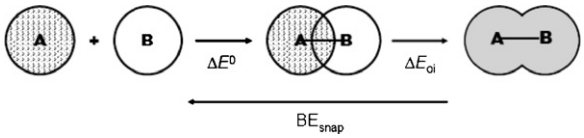

Fig. 8. The bond snapping energy and the two-step process of bond formation.

3.5.1. Energy decomposition

An energy decomposition scheme, which is widely used in the analysis of chemical bonding and that has found application also for NHC complexes, is based on ideas developed by Morokuma [133] and by Ziegler and Rauk [134,135]. This model, often referred to as energy decomposition analysis EDA, is well described in the literature [136,137], but since we will discuss EDA results in greater detail, we briefly summarize the gist of this method.

In order to analyze a chemical bond in a molecule, one separates the chemical entity into two fragments A and B that result from cleavage of the bond to be analyzed. Then, one examines the energy of interconnection of the two fragments A and B associated with formation of the final molecule. The fragments A and B posses the local equilibrium geometry of the final molecule, and have the electronic structure that is required for bond formation. The focus of such a bonding analysis is the instantaneous interconnection energy, which is the energy difference between the molecule and the fragments in the frozen geometry of the compound, having the electronic reference state of the final molecule. The energy associated with the bond formation process from suitably prepared fragments is related to the bond snapping energy, BE_{snap} [138,139].

Bond formation can be envisioned as a two-step process. First, the fragments are brought together from infinite separation to adapt the geometry of the final molecule, and each fragment *reacts* to the presence of its counter-fragment. The energy associated with the first step is usually called the *steric interaction* energy ΔE^0. Then, the fragments *interact* and utilize the full variational space of all orbitals available, occupied as well as virtual, to relax to the fully converged ground-state wave function of the total molecule. The energy associated with the second step is referred to as the *orbital interaction* energy ΔE_{oi}. Thus, the bond snapping energy BE_{snap} writes as in Eq. (3):

$$BE_{snap} = -[\Delta E^0 + \Delta E_{oi}] \quad (3)$$

The two-step bond formation process is schematically illustrated in Fig. 8. The bond-snapping energy BE_{snap} actually refers to the initial step in which the chemical entity is set up for bond analysis, and the bond to be analyzed is cleaved or "snapped".

BE_{snap} can be used to calculate the bond dissociation energy, D_e, by adding a preparation energy term ΔE_{prep}. ΔE_{prep} is the energy necessary to promote the fragments from their equilibrium geometry to the geometry in the compound, and if required, to electronically excite the fragments from their electronic ground-states to the reference states in the molecule. It is to achieve compatibility with bond dissociation energies that the bond snapping energy is defined as the negative value of the sum of its contributors;

a positive value of BE_{snap} indicates a stable bond. Although the bond snapping energy BE_{snap} does not always correlate with bond dissociation energies, since reorganization and relaxation of the fragments are not taken into account, it is closely related to bond enthalpy terms, which in turn provide a good approximation to bond strength values [140].

3.5.2. The steric interaction term

The steric interaction energy ΔE^0 is obtained from the energy E^0 of the wave function ψ^0, see Eq. (4), which is constructed as the antisymmetrized (A) and renormalized (N) product of the wave functions ψ^A and ψ^B of the fragments A and B:

$$\psi^0 = A \cdot N \cdot \{\psi^A \psi^B\}; \quad E^0 = \left\langle \psi^0 | H | \psi^0 \right\rangle \tag{4}$$

We note that the steric interaction energy is unambiguously defined as in Eq. (5) [141]:

$$\Delta E^0 = E^0 - E^A - E^B \tag{5}$$

The steric interaction energy consists of two components, namely the electrostatic interaction energy between the fragments ΔE_{elstat} and the repulsive interactions ΔE_{Pauli} as in Eq. (6).

$$\Delta E^0 = \Delta E_{elstat} + \Delta E_{Pauli} \tag{6}$$

ΔE_{elstat} can be conceived as the classical electrostatic interaction of the nuclear charges and unperturbed electronic charge distribution of one fragment with those of the other fragment, with both fragments being at their final position. ΔE_{Pauli} refers to the repulsive interactions between the fragments, which are caused by the fact that two electrons with the same spin cannot occupy the same region in space. In the framework of density functional theory, it is calculated by enforcing the Kohn–Sham determinant on the superimposed fragments to obey the Pauli principle by antisymmetrization and renormalization. ΔE_{Pauli} comprises the three- and four electron destabilizing interactions between occupied orbitals. It is ΔE_{Pauli} and not the steric interaction term ΔE^0 that corresponds to the intuitive concept of steric repulsion [142–144], widely used in chemistry.

The clear distinction between steric interaction and steric repulsion is often lost in recent applications of the EDA scheme. For example, in reference to early applications of EDA [145,146], it has been stated that it was only "later recognized that ΔE^0 has nothing to do with the loosely defined steric interaction that is often used to explain the repulsive interactions" [116]. However, it was clear from the beginning that ΔE^0 is the energy of interaction when no electron transfer can take place, and that ΔE^0 may be attractive or repulsive [135]. The attractive or repulsive nature of ΔE^0 is determined by the relative value of attractive electrostatic interaction and Pauli repulsion. We re-iterate the fact that it is ΔE_{Pauli} and not ΔE^0 which corresponds to the qualitative idea of repulsive steric interaction. In view of the clear definition of steric interaction, the claim that a negative ΔE^0 "leads to a non-physical description of attractive steric interactions" [116] remains largely unsupported.

3.5.3. The orbital interaction term

The stabilizing orbital interaction term, ΔE_{oi}, is the result from the second step of the bond formation process, when the constituting fragment orbitals relax to the fully converged ground-state wave function of the total molecule. This term accounts for charge transfer processes, which are interactions between occupied orbitals on one molecular fragment and unoccupied orbitals on the other, as well as polarization effects, the mixing of occupied and virtual orbitals on one fragment [133].

The total orbital interaction energy ΔE_{oi} can further be broken down into contributions from the orbital interactions within the various irreproducible representations Γ of the overall symmetry group of the system, see Eq. (7) [135]:

$$\Delta E_{oi} = \sum_{\Gamma} \Delta E_{oi}^{\Gamma} \tag{7}$$

For the M—(NHC) bond, such decomposition allows one to extract values for σ as well as π-contributions to ΔE_{oi}. The relevant orbital interactions that dominate the M—(NHC) bond are depicted in Fig. 9.

The σ-contribution ΔE_{oi}^{σ} can be classified as σ-*donation* from the NHC-ligand to the transition metal center. The π-contribution ΔE_{oi}^{π} on the other hand is characterized by an interplay of π-*donation* from the NHC-ligand to the transition metal center and of π^*-*backdonation* from the metal to the ligand. Although the backdonation is the major contribution to the π-interaction, π-donation is not negligible and is a relevant factor that determines the nature of the M—(NHC) bond.

Constrained space orbital variation (CSOV) calculations utilizing a suitable division of the variational space make it possible to differentiate between these two interactions [147,148]. In particular, in order to assess the contribution of π^*-backdonation, the bond decomposition analysis excludes those virtual orbitals on the M fragment from the variational space, which belong to the irreducible representation that characterizes the π-bond. The π-contribution of the orbital interaction energy is now associated solely with interunit M to NHC π^*-backdonation, $\Delta E_{oi}^{\Pi}(M \rightarrow NHC)$. Similarly, the amount of π-donation $\Delta E_{oi}^{\Pi}(NHC \rightarrow M)$ is determined in calculations explicitly excluding all virtual orbitals of the NHC ligand from the variational space, which belong to the irreducible representation that characterizes the π-bond. The sum of these two individual contributions differs slightly from ΔE_{oi}^{π} by a small synergic contribution. Different synergic as well as residual contributions to the orbital interaction energy may arise from different choices of variational space partitioning [149], but the presence of synergic and residual contributions does not affect the bonding picture that is obtained from CSOV calculations.

3.5.4. Decomposition schemes

From the discussion above, it becomes evident that the bond snapping energy BE_{snap} is comprised of three major components, namely the orbital interaction, electrostatic interaction, and Pauli repulsion as in Eq. (8):

$$BE_{snap} = -[\Delta E_{oi} + \Delta E_{elstat} + \Delta E_{Pauli}] \tag{8}$$

The different contributions to the bond snapping energy are often grouped together as to emphasize different aspects of the chemical bond [150]. As already discussed, Pauli repulsion and electrostatic interaction are commonly combined into the steric interaction term ΔE^0, Eq. (6). The resulting partitioning scheme, Eq. (3), follows the two-step process of first reacting and then interacting fragments, and puts special emphasis on the role of orbital interactions.

To stress the importance of electrostatic interaction for chemical bonding, one might merge the terms for Pauli repulsion and orbital interaction into a combined orbital term ΔE^{orb} [151]. This definition can be justified keeping in mind that both terms basically stem from interactions between orbitals on the two different fragments; be it repulsive or attractive. The bond snapping energy then writes as in Eq. (9):

$$BE_{snap} = -[\Delta E^{orb} + \Delta E_{elstat}] \tag{9}$$

Realizing that both electrostatic as well as orbital interactions constitute attractive bonding forces, these two terms might be analyzed together as combined attractive interaction ΔE^{attr}, and one

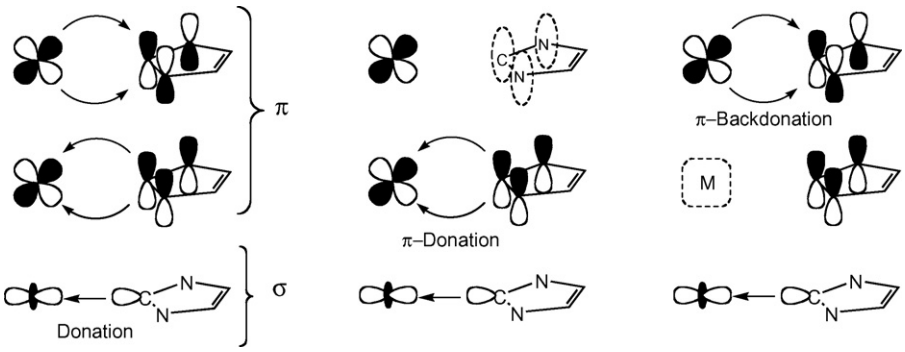

Fig. 9. Orbital interactions in the M–(NHC) bond, and CSOV-partitioning for π donation and π backdonation.

obtains the expression of Eq. (10) for the bond snapping energy:

$$BE_{snap} = -[\Delta E^{attr} + \Delta E_{Pauli}] \quad (10)$$

This analysis evaluates the role and importance of attractive bonding forces due to electrostatic interactions, but it also allows for a suitable comparison of attractive and repulsive forces that govern a chemical bond.

3.6. Balancing of the σ, π and π* contributions: general trends in M–(NHC) bonding

It is instructive to summarize the main results of EDA analyses of M—(NHC) bonding, before engaging in a comprehensive analysis of orbital interactions. Values of the bond snapping energy BE_{snap} span a large spectrum of about 70 kcal/mol, ranging from 98 kcal/mol for cationic gold complexes to 26 kcal/mol for anionic titanium complexes. The progression observed for the bond snapping energy BE_{snap} is neither paralleled in the electrostatic interaction ΔE_{elstat} nor in orbital interaction ΔE_{oi}, the two attractive components of the bond snapping energy. Also the Pauli repulsion ΔE_{Pauli} does not follow the ranking scheme observed for the bond snapping energies. It is clear that the M—(NHC) bond is characterized by the subtle interplay of various bond factors.

If one follows a bond partitioning according to steric interaction and orbital interaction, it is evident that ΔE_{oi} provides the major bonding interaction. The steric term is responsible for a fine-tuning of the relative bond strength, by providing either secondary attractive or secondary repulsive interactions. Various trends can be established for the M—(NHC) bond:

1. For cationic systems, electrostatic interactions as attractive bonding forces constitutes a most important factor. In such systems the steric interaction ΔE^0 is stabilizing, indicating that attractive electrostatic interaction outweighs Pauli repulsion.
2. Anionic systems form weaker bonds than cationic or neutral systems. Here, the steric interaction ΔE^0 contributes a fairly large destabilizing contribution, dominated by Pauli repulsion.
3. Systems with higher formal d electron count form stronger bonds. This observation reflects trends observed both in the orbital interaction term as well as in the electrostatic interaction.
4. Additional ligands L of L_nM–NHC complexes that deplete electron density at the transition metal center due to π-acceptance lead to a decrease in attractive orbital interaction ΔE_{oi} and at the same time to a decrease in Pauli repulsion ΔE_{Pauli}.
5. Additional ligands L of L_nM–NHC complexes that enhance electron density at the transition metal center due to secondary π-interactions lead to an increase in attractive orbital interaction ΔE_{oi} and at the same time to an increase in repulsive interaction ΔE_{Pauli}.

Trends in orbital interaction are often mirrored in Pauli repulsion. It is also evident that the various contributions to ΔE_{oi} have to be considered independently. The detailed make-up of the M–(NHC) provides valuable insights for an efficient bond tuning. At the same time, the nature of the M—(NHC) bond reveals little differences when "normal" NHC systems are compared with "anormal" ones [116]. It is also noteworthy that saturated and unsaturated NHC ligands hardly differ in their electronic ligand properties [152]. Thus, *qualitative* bonding patterns established for one class of NHC ligand yield a general bond picture for whole NHC family. However, as we have seen, the fine *quantitative* differences in M—(NHC) bonding give rise to a multitude of different chemical utilizations and applications.

3.6.1. σ and π contributions to the M—(NHC) bond

Computational evidence for significant metal–carbene π-interaction was first reported for a tripodal N-heterocyclic carbene ligand [64,112], and it was found that π-bonding amounts to at least 15% of the total orbital interaction energy. Since then, a vast number of M–(NHC) complexes has been subjected to a detailed σ/π-partitioning analysis [115,116,124,128,131]. That π-bonding in M–(NHC) complexes is more than a conceptual consideration was proven by spectroscopic and crystallographic analyses of M–(NHC) complexes, which clearly provided experimental evidence as well for M → NHC π*-backdonation interactions [122].

An extensive study of 36 model M–(NHC) complexes, which includes systems in which the formal d-electron count for the transition metal amounts to d^0, d^4, d^6, d^8, and d^{10}, and which further includes cationic as well as anionic compounds serves as comprehensive data base for establishing trends in σ- and π-bonding of the M–(NHC) bond [115]. The fact that the model systems were based on crystal structures of NHC complexes of copper [153], silver [154], gold [155–157], nickel [158], palladium [159,160], platinum [161], iron [162], ruthenium [163], osmium [164], chromium [117], molybdenum [165], tungsten [166], vanadium [114], titanium [89], and hafnium [167] lends credibility to the validity of the set of selected molecules for establishing general M–(NHC) bonding trends. Inspection of the data reveals that the ratio of σ- and π-contributions to the orbital interaction energy, as well as the ratio of donation and backdonation of the π-component of ΔE_{oi} correlates with the formal d-electron count of the transition metal (Table 4).

In accord with intuitive qualitative considerations, the amount of metal to ligand π-interaction increases with increasing d-electron count, and reaches an average 20% contribution for d^{10} systems. Even for the d^0 systems, one sees an average π-contribution of 10%. More specifically, a cationic Ti–NHC complex which in a previous calculation has been described as a pure σ-donor [89], possesses 17% π-bonding character. The bonding in M–(NHC) is complex, and simplifying classifications such as "pure"

Table 4
Average percent σ and π contributions of ΔE_{oi}^{σ} and ΔE_{oi}^{π} to the orbital interaction energy, and average percent contributions due to π*-backdonation and π-donation to ΔE_{oi}^{π}

	Formal d electron count				
	0	4	6	8	10
ΔE_{oi}^{σ}	90	88	86	85	80
ΔE_{oi}^{π}	10	12	14	15	20
ΔE_{oi}^{π} (π*-backdonation)	65	70	77	82	90
ΔE_{oi}^{π} (π-donation)	35	30	23	18	10

Averages are based on data for 36 M–(NHC) model complexes compiled in ref. [115].

σ-donor do not capture the subtleties of the M—(NHC) bond. The same holds true for the use of a term such as "negligible" to describe the π-bonding in metal NHC complexes. While the argument that 10% of bonding is "negligible" is open for discussion, such simplification would certainly overlook the exact nature of the M—(NHC) bond, as well as the potential role of metal–carbene π*-backdonation in the diverse NHC chemistry.

What the data of Table 4 clearly indicate is the fact that the role of ligand to metal donation increases in importance with decreasing d-electron count. Complexes with formal d-electron count of zero not only display the largest σ-donation component for the orbital interaction energy, even the π component has a sizable donation contribution of 35%. The role of π-donation decreases with increasing d-electron count, and of the model compounds, it is the set of d^{10} complexes for which π*-backdonation is most significant.

3.6.2. Electrostatic contributions to the M–(NHC) bond

The role and importance of electrostatic contributions for a description of chemical bonding of transition metal complexes that goes beyond simplistic σ/π orbital considerations has recently been illustrated for "non-classical" carbonyl complexes [168]. It became clear that the charge of the transition metal center determines the magnitude and influence of electrostatic interaction for ligand bonding to transition metal centers, and that this influence is most pronounced for cationic systems. Recent EDA analysis of M–(NHC) systems put a special emphasis on ΔE_{elstat}, but fail to address the function of the transition metal center for electrostatic interaction [116,124]. Here, the role of electrostatic interaction is often analyzed by a breakdown of the attractive energy term ΔE^{attr}, Eq. (9). The importance of electrostatic interaction then is judged in terms of its contribution to the total attractive interaction energy, $\Delta E_{elstat}^{\%attr}$. This breakdown, however, is not easy to interpret. Not only are the underlying forces for ΔE_{elstat}, and ΔE_{oi} different in their origin, but also are the absolute values of ΔE_{elstat}, and ΔE_{oi} not to be put on equal footing; ΔE_{elstat} in general is significantly larger than ΔE_{oi}. For M–(NHC) complexes as well as for related Fischer carbene complexes, $\Delta E_{elstat}^{\%attr}$ in general is 60% and larger, and reaches values close to 80%. Such an analysis suggests that ΔE_{elstat}, constitutes the main component responsible for the metal to ligand bond. Trends in ΔE_{elstat} are superimposed by trends in ΔE_{oi}, which makes it difficult to draw unambiguous conclusions from such a partitioning.

A partioning that provides a clearer picture of the role of ΔE_{oi} for M–(NHC) bonding puts the total bond energy in relation to the electrostatic component, $-BE_{snap}^{\%elstat}$, and the larger the value of $-BE_{snap}^{\%elstat}$, the larger the influence of ΔE_{elstat} on the chemical bond.

A set of model M–(NHC) complexes, for which EDA data are available in the literature, has been chosen to illustrate the decomposition in terms of $-BE_{snap}^{\%elstat}$. For the sake of comparison, two Fischer-type carbene complexes are also included. These 29 molecules are illustrated in Chart 12. The results for the model complexes are displayed in Fig. 10. $-BE_{snap}^{\%elstat}$ values span a large

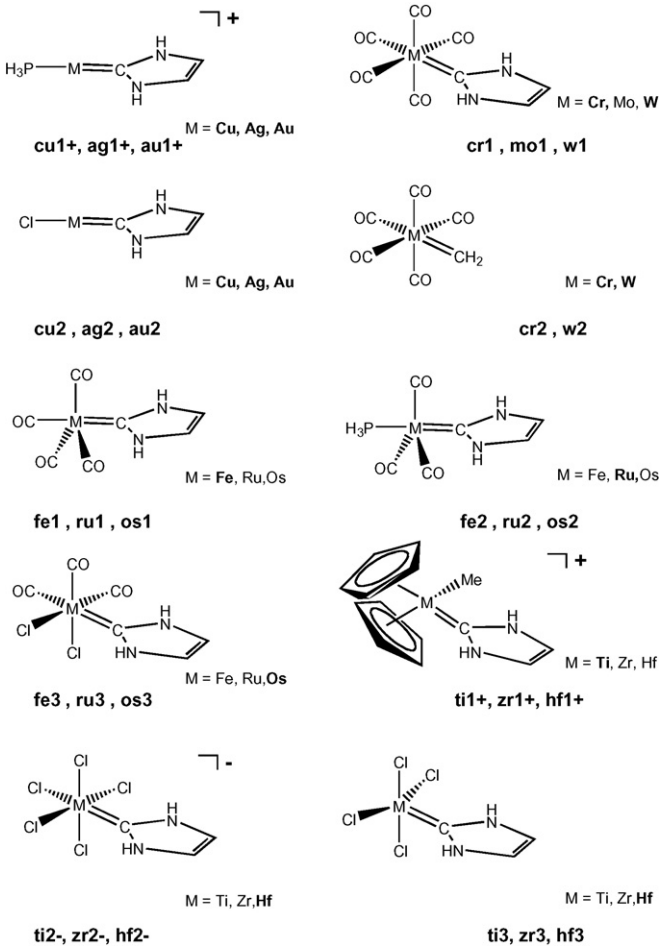

Chart 12.

range, roughly ranging from 25% up to 65%. We note that the Fischer carbene complexes (**cr2**, **w2**) do not occupy a special position within the $-BE_{snap}^{\%elstat}$ ranking, but fall in line of the general progression for all carbene complexes of the chosen model set. Although differences between Fischer carbenes and N-heterocyclic carbenes are found, the NHC ligands undergoing stronger electrostatic interactions presumably due to the presence of more electronegative N-atoms, this analysis does not promote the notion that ΔE_{elstat} is significantly different in NHC ligands when compared to Fischer carbene ligands.

For anionic complexes, ΔE_{elstat} is only a secondary bonding component. The same holds true for complexes where additional lone-pair ligands at the [M] moiety such as Cl^- increase the electron density of the transition metal complex (e.g. **fe3**, **ru3**, **os3**). For neutral d^0-complexes and cationic complexes ΔE_{elstat} increasingly gains importance, and reaches contributions exceeding 60%. At the same time, this analysis provides only insight into the character of the M—(NHC) bond, but does not allow for a prediction of relative bond strengths. For example, both cationic complexes [Ti^+]–NHC **ti1**+ and [Cu^+]–NHC **cu1**+ display a $-BE_{snap}^{\%elstat}$ contribution of 60%. Yet, the bond snapping energy for the copper complex is 30 kcal/mol larger than for the titanium complex. As mentioned before, the M—(NHC) bond is characterized by a subtle interplay of the various contributing factors.

Electrostatic contributions are certainly of importance for the M—(NHC) bond as they counteract the steric repulsion in the first step of bond formation. Electrostatic contributions might provide additional bond stability, but they are not easily accessible when

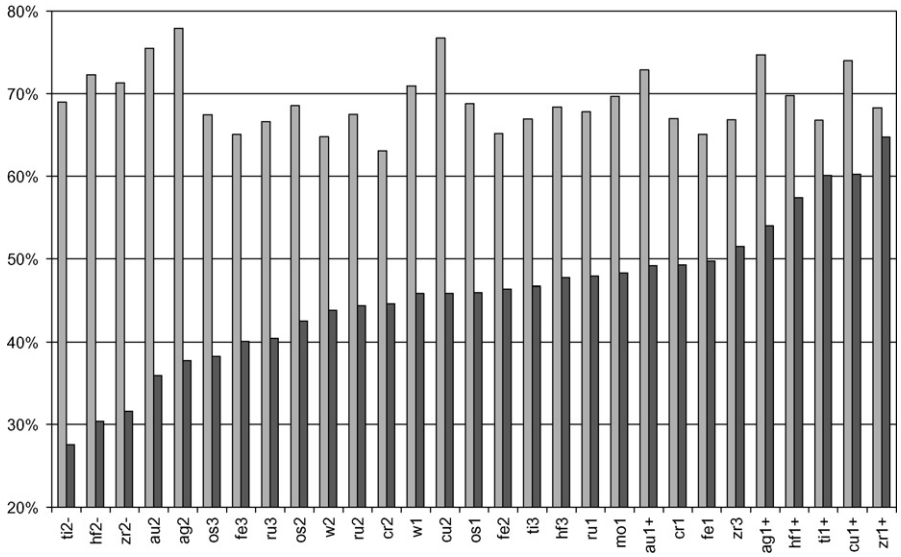

Fig. 10. $-BE^{\%elstat}_{snap}$ contributions (black bars) and $\Delta E^{\%attr}_{elstat}$ contributions (grey bars) to the metal–ligand bond for 29 model complexes. Data compiled from refs. [37,115,116].

a fine-tuning of M—(NHC) bond or an optimization of the electronic properties of N-heterocyclic carbene complexes is sought. It is variation in σ-donation and in π-bonding that provides an experimental entry into modifying the reactivity and chemistry of M–(NHC) complexes.

3.7. Steric effects in the M—(NHC) bond

The bond dissociation energies of NHC, calculated for a series of Ru and Ni complexes, are reported in Table 2. As discussed in Section 3.1, the relative strength of the M—(NHC) bond is clearly dependent on the steric properties of the NHC-ligands in the crowded $Cp^*Ru(NHC)Cl$ and $Ni(CO)_3(NHC)$ complexes. In the former class, the BDE of the NHC ligands depends strongly on the bulkiness of the groups in the *ortho* position of the aromatic rings of the NHC ligand. Largest BDEs are calculated for complexes without alkyl groups in the *ortho* positions, such as the ITol, decreases of roughly 7–8 kcal/mol in complexes bearing NHC ligands with Me groups in the *ortho* position of the aromatic substituents on the N atoms, such as with the IMes and SIMes ligands, and further decreases by another 7–8 kcal/mol in complexes bearing NHC ligands with *i*-Pr groups in these positions, such as with the IPr and SIPr ligands.

To quantify these steric factors the BDEs of $Cp^*Ru(NHC)Cl$ systems have been plotted versus the percent of buried volume, $\%V_{Bur}$, in Fig. 11. The $\%V_{Bur}$ which is the fraction of the volume of a sphere centered on the metal, buried by overlap with atoms of the various NHC ligands. The volume of this sphere would represent the space around the metal atom that must be shared by the different ligands upon coordination [33]. The plot of Fig. 11 shows a linear correlation between the experimental BDEs and the $\%V_{Bur}$, which clearly indicates that the BDEs are essentially controlled by the steric requirements of the ligands, and that $\%V_{Bur}$, although a very simple and intuitive molecular descriptor, is able to capture the different steric requirements of the different ligands.

Focusing on the Ni-based complexes, their stability depends dramatically on the bulkiness of N-substituents of the NHC ligands. With the less bulky IMes and SIMes NHC ligands the saturated $Ni(CO)_3(NHC)$ complexes are stable, whereas with the bulkier IAd and ItBu NHC ligands the 18e $Ni(CO)_3(NHC)$ complexes are unstable, and the unsaturated 16e $Ni(CO)_2(NHC)$ complexes are instead formed. The instability of the saturated $Ni(CO)_3(NHC)$ complexes

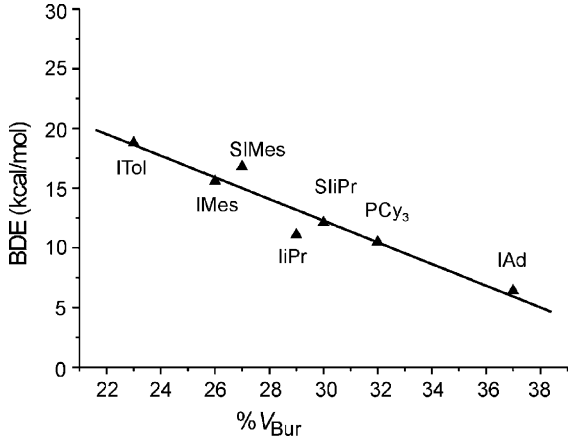

Fig. 11. Experimental BDE (kcal/mol) vs. steric parameter ($\%V_{Bur}$) in the $Cp^*Ru(L)Cl$ systems, from ref. [63].

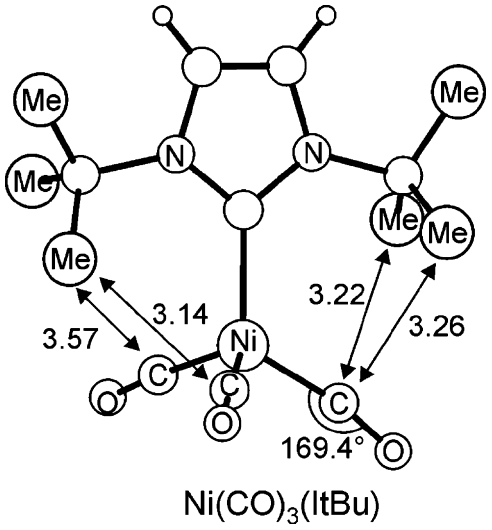

Fig. 12. DFT geometry of the $Ni(CO)_3$ItBu complex, from ref. [65]. Short distances in Å.

with bulky NHC ligands, such as IAd and ItBu, is essentially due to strong steric interactions between the NHC ligands and the CO ligands. This was supported by the geometrical inspection of the DFT optimized $Ni(CO)_3$(ItBu) complex, see, which presents several short distances between the *t*-Bu group and the CO ligands, relative to unsaturated but sterically unstrained $Ni(CO)_2$(ItBu) complex. The strong steric interactions in $Ni(CO)_3$(ItBu) result in a deviation out-of-axis by 11° of one of the Ni–C–O angles. Differently, the $Ni(CO)_3$(IiPr) of Fig. 12 is characterized by very few short distances between the NHC ligand and the CO molecules, which explains its stability.

4. Final remarks

The sparkling discovery of the first stable crystalline NHC in 1991 provided the chemical community with a new class of versatile ligands whose steric and electronic properties can be tuned almost at wish. This variability spurred extensive investigations in the field, to understand the details of NHCs as ligands as well as of the M—(NHC) bond, and how the unique features of NHCs result in new and sometime unpredictable catalysis. It is clear that the end of the story has not been written yet, and many more exciting insights will come from both the experimental and theoretical communities.

Acknowledgements

L.C. thanks the MIUR of Italy, the INSTM (Cineca Grant), and the Regione Campania (Progetto Legge 5 2005) for financial support. A.P. thanks the Spanish Ministerio de Educación y Ciencia (MEC) for a post-doctoral grant. KemKom acknowledges Ms. Chiara Lui for constructive criticism and creative comments.

References

[1] H.W. Wanzlick, H.J. Kleiner, Angew. Chem. 73 (1961) 493.
[2] H.-W. Wanzlick, Angew. Chem. Int. Ed. Engl. 1 (1962) 75.
[3] K. Öfele, J. Organomet. Chem. 12 (1968) P42.
[4] H.W. Wanzlick, H.-J. Schönherr, Angew. Chem. Int. Ed. Engl. 7 (1968) 141.
[5] K. Öfele, M. Herberhold, Angew. Chem. Int. Ed. Engl. 9 (1970) 739.
[6] A.J. Arduengo, R.L. Harlow, M. Kline, J. Am. Chem. Soc. 113 (1991) 361.
[7] A.J. Arduengo, M. Kline, J.C. Calabrese, F. Davidson, J. Am. Chem. Soc. 113 (1991) 9704.
[8] A.J. Arduengo, H.V.R. Dias, R.L. Harlow, M. Kline, J. Am. Chem. Soc. 114 (1992) 5530.
[9] A.J. Arduengo, F. Davidson, H.V.R. Dias, J.R. Goerlich, D. Khasnis, W.J. Marshall, T.K. Prakasha, J. Am. Chem. Soc. 119 (1997) 12742.
[10] A.J. Arduengo, J.R. Goerlich, W.J. Marshall, J. Am. Chem. Soc. 117 (1995) 11027.
[11] T. Weskamp, W.C. Schattenmann, M. Spiegler, W.A. Herrmann, Angew. Chem. Int. Ed. 37 (1998) 2490.
[12] M. Scholl, S. Ding, C.W. Lee, R.H. Grubbs, Org. Lett. 1 (1999) 953.
[13] J. Huang, E.D. Stevens, S.P. Nolan, J.L. Peterson, J. Am. Chem. Soc. 121 (1999) 2674.
[14] A.H. Hoveyda, R.R. Schrock, Chem. Eur. J. 7 (2001) 945.
[15] A. Fürstner, Angew. Chem. Int. Ed. 39 (2000) 3012.
[16] T.M. Trnka, R.H. Grubbs, Acc. Chem. Res. 34 (2001) 18.
[17] L. Jafarpour, S.P. Nolan, J. Organomet. Chem. 617–618 (2001) 17.
[18] L.D. Vázquez-Serrano, B.T. Owens, J.M. Buriak, Chem. Commun. (2002) 2518.
[19] H.M. Lee, T. Jiang, E.D. Stevens, S.P. Nolan, Organometallics 20 (2001) 1255.
[20] A.C. Hillier, H.M. Lee, E.D. Stevens, S.P. Nolan, Organometallics 20 (2001) 4246.
[21] G.A. Grasa, M.S. Viciu, J. Huang, S.P. Nolan, J. Org. Chem. 66 (2001) 7729.
[22] G.A. Grasa, M.S. Viciu, J. Huang, C. Zhang, M.L. Trudell, S.P. Nolan, Organometallics 21 (2002) 2866.
[23] N. Marion, O. Navarro, J. Mei, E.D. Stevens, N.M. Scott, S.P. Nolan, J. Am. Chem. Soc. 128 (2006) 4101.
[24] N. Marion, P. de Frémont, G. Lemière, E.D. Stevens, L. Fensterbank, M. Malacria, S.P. Nolan, Chem. Commun. (2006) 2048.
[25] A. Correa, N. Mario, L. Fensterban, M. Malacria, S.P. Nolan, L. Cavallo, Angew. Chem. Int. Ed. 47 (2008) 718.
[26] M.C. Perry, K. Burgess, Tetrahedron: Asymmetry 14 (2003) 951.
[27] T.W. Funk, J.M. Berlin, R.H. Grubbs, J. Am. Chem. Soc. 128 (2006) 1840.
[28] T.J. Seiders, D.W. Ward, R.H. Grubbs, Org. Lett. 3 (2001) 3225.
[29] J.J. Van Veldhuizen, S.B. Garber, J.S. Kingsbury, A.H. Hoveyda, J. Am. Chem. Soc. 124 (2002) 4954.
[30] S. Diez-Gonzalez, S.P. Nolan, Coord. Chem. Rev. 251 (2007) 874.
[31] F. Glorius, Top. Organomet. Chem. 21 (2007) 1.
[32] R.W. Alder, M.E. Blake, L. Chaker, J.N. Harvey, F. Paolini, J. Schutz, Angew. Chem. Int. Ed. 43 (2004) 5896.
[33] L. Cavallo, A. Correa, C. Costabile, H. Jacobsen, J. Organomet. Chem. 690 (2005) 5407.
[34] D. Bourissou, O. Guerret, F.P. Gabbaï, G. Bertrand, Chem. Rev. 100 (2000) 39.
[35] C.M. Crudden, D.P. Allen, Coord. Chem. Rev. 248 (2004) 2247.
[36] V. Nair, S. Bindu, V. Sreekumar, Angew. Chem. Int. Ed. 43 (2004) 5130.
[37] G. Frenking, M. Solà, S.F. Vyboishchikov, J. Organomet. Chem. 690 (2005) 6178.
[38] W.A. Herrmann, Angew. Chem. Int. Ed. 41 (2002) 1291.
[39] C. Heinemann, W. Thiel, Chem. Phys. Lett. 217 (1994) 11.
[40] R. Hoffmann, J. Am. Chem. Soc. 90 (1968) 1475.
[41] M.-D. Su, S.-Y. Chu, Chem. Phys. Lett. 308 (1999) 283.
[42] A.J. Arduengo, H. Bock, H. Chen, M. Denk, D.A. Dixon, J.C. Green, W.A. Herrmann, N.L. Jones, M. Wagner, R. West, J. Am. Chem. Soc. 116 (1994) 6641.
[43] F. Ullah, G. Bajor, T. Veszpremi, P.G. Jones, J.W. Heinicke, Angew. Chem. Int. Ed. 46 (2007) 2697.
[44] C. Heinemann, T. Muller, Y. Apeloig, H. Schwarz, J. Am. Chem. Soc. 118 (1996) 2023.
[45] C. Boehme, G. Frenking, J. Am. Chem. Soc. 118 (1996) 2039.
[46] S.P. Nolan (Ed.), N-heterocyclic Carbenes in Synthesis, Wiley-VCH, 2006.
[47] F. Glorius, N-heterocyclic Carbenes in Transition Metal Catalysis, 2007.
[48] A.J. Arduengo, R. Krafczyk, A.J. Arduengo, R. Krafczyk, Chem. Unserer Zeit 32 (1998) 6.
[49] W.A. Herrmann, C. Kocher, Angew. Chem. Int. Ed. Engl. 36 (1997) 2163.
[50] M. Regitz, Angew. Chem. Int. Ed. Engl. 35 (1996) 725.
[51] E.A. Carter, W.A. Goddard III, J. Phys. Chem. 90 (1986) 998.
[52] M.J. Cheng, C.H. Hu, Chem. Phys. Lett. 322 (2000) 83.
[53] M.J. Cheng, C.H. Hu, Chem. Phys. Lett. 349 (2001) 477.
[54] L. Nyulászi, T. Veszprémi, A. Forró, Phys. Chem. Chem. Phys. 2 (2000) 3127.
[55] D.C. Graham, K.J. Cavell, B.F. Yates, J. Phys. Org. Chem. 18 (2005) 298.
[56] M.K. Denk, A. Hezarkhani, F.L. Zheng, Eur. J. Inorg. Chem. (2007) 3527.
[57] A. Poater, F. Ragone, S. Giudice, C. Costabile, R. Dorta, S.P. Nolan, L. Cavallo, Organometallics 27 (2008).
[58] C.A. Tolman, Chem. Rev. 77 (1977) 313.
[59] Y.F. Liu, P.E. Lindner, D.M. Lemal, J. Am. Chem. Soc. 121 (1999) 10626.
[60] W.A. Herrmann, C. Kocher, L.J. Goossen, G.R.J. Artus, Chem. Eur. J. 2 (1996) 1627.
[61] N. Wiberg, Angew. Chem. Int. Ed. Engl. 7 (1968) 766.
[62] T. Ziegler, Chem. Rev. 91 (1991) 651.
[63] A.C. Hillier, W.J. Sommer, B.S. Yong, J.L. Petersen, L. Cavallo, S.P. Nolan, Organometallics 22 (2003) 4322.
[64] X.L. Hu, I. Castro-Rodriguez, K. Olsen, K. Meyer, Organometallics 23 (2004) 755.
[65] R. Dorta, E.D. Stevens, N.M. Scott, C. Costabile, L. Cavallo, C.D. Hoff, S.P. Nolan, J. Am. Chem. Soc. 127 (2005) 2485.
[66] R.A. Kelly III, H. Clavier, S. Giudice, N.M. Scott, E.D. Stevens, J. Bordner, I. Samardjiev, C.D. Hoff, L. Cavallo, S.P. Nolan, Organometallics 27 (2008) 202.
[67] E. van Lenthe, A.E. Ehlers, E.J. Baerends, J. Chem. Phys. 110 (1999) 8943.
[68] E. van Lenthe, E.J. Baerends, J.G. Snijders, J. Chem. Phys. 99 (1993) 4597.
[69] E. van Lenthe, E.J. Baerends, J.G. Snijders, J. Chem. Phys. 101 (1994) 9783.
[70] S. Fantasia, J.L. Petersen, H. Jacobsen, L. Cavallo, S.P. Nolan, Organometallics 26 (2007) 5880.
[71] J.C. Green, R.G. Scurr, P.L. Arnold, F.G.N. Cloke, Chem. Commun. (1997) 1963.
[72] G. Frison, A. Sevin, J. Chem. Soc., Perkin Trans. 2 (2002) 1692.
[73] N. Kuhn, T. Kratz, D. Blaser, R. Boese, Chem. Ber. 128 (1995) 245.
[74] N. Kuhn, G. Henkel, T. Kratz, J. Kreutzberg, R. Boese, A.H. Maulitz, Chem. Ber. Recl. 126 (1993) 2041.
[75] A.J. Arduengo, H.V.R. Dias, J.C. Calabrese, F. Davidson, J. Am. Chem. Soc. 114 (1992) 9724.
[76] X.W. Li, J.R. Su, G.H. Robinson, Chem. Commun. (1996) 2683.
[77] H. Nakai, Y.J. Tang, P. Gantzel, K. Meyer, Chem. Commun. (2003) 24.
[78] W.M. Boesveld, B. Gehrhus, P.B. Hitchcock, M.F. Lappert, P.V. Schleyer, Chem. Commun. (1999) 755.
[79] R.W. Alder, M.E. Blake, C. Bortolotti, S. Bufali, C.P. Butts, E. Linehan, J.M. Oliva, A.G. Orpen, M.J. Quayle, Chem. Commun. (1999) 241.
[80] A.J. Arduengo, H.V.R. Dias, F. Davidson, R.L. Harlow, J. Organomet. Chem. 462 (1993) 13.
[81] A.J. Arduengo, F. Davidson, R. Krafczyk, W.J. Marshall, M. Tamm, Organometallics 17 (1998) 3375.
[82] H. Schumann, J. Gottfriedsen, M. Glanz, S. Dechert, J. Demtschuk, J. Organomet. Chem. 617 (2001) 588.
[83] H. Schumann, M. Glanz, J. Winterfeld, H. Hemling, N. Kuhn, T. Kratz, Angew. Chem. Int. Ed. Engl. 33 (1994) 1733.
[84] H. Schumann, M. Glanz, J. Gottfriedsen, S. Dechert, D. Wolff, Pure Appl. Chem. 73 (2001) 279.
[85] A.J. Arduengo, M. Tamm, S.J. McLain, J.C. Calabrese, F. Davidson, W.J. Marshall, J. Am. Chem. Soc. 116 (1994) 7927.
[86] R.D. Fischer, Angew. Chem. Int. Ed. Engl. 33 (1994) 2165.
[87] W.A. Herrmann, O. Runte, G. Artus, J. Organomet. Chem. 501 (1995) C1.
[88] N. Fröhlich, U. Pidun, M. Stahl, G. Frenking, Organometallics 16 (1997) 442.
[89] M. Niehues, G. Erker, G. Kehr, P. Schwab, R. Fröhlich, O. Blacque, H. Berke, Organometallics 21 (2002) 2905.
[90] M. Niehues, G. Kehr, G. Erker, B. Wibbeling, R. Fröhlich, O. Blacque, H. Berke, J. Organomet. Chem. 663 (2002) 192.

[91] W.A. Herrmann, K. Öfele, M. Elison, F.E. Kuhn, P.W. Roesky, J. Organomet. Chem. 480 (1994) C7.
[92] G.B. Nikiforov, H.W. Roesky, P.G. Jones, J. Magull, x.f. rg, A. Ringe, R.B. Oswald, Inorg. Chem. 47 (2008) 2171.
[93] M.T. Lee, C.H. Hu, Organometallics 23 (2004) 976.
[94] A.J. Arduengo, S.F. Gamper, J.C. Calabrese, F. Davidson, J. Am. Chem. Soc. 116 (1994) 4391.
[95] J.S. Slater, The Calculation of Molecular Orbitals, Wiley, 1979.
[96] E.F. Penka, C.W. Schlaepfer, M. Atanasov, M. Albrecht, C. Daul, J. Organomet. Chem. 692 (2007) 5709.
[97] L. Ray, M.M. Shaikh, P. Ghosh, Dalton Trans. (2007) 4546.
[98] C. Boehme, G. Frenking, Organometallics 17 (1998) 5801.
[99] S.F. Vyboishchikov, G. Frenking, Chem. Eur. J. 4 (1998) 1428.
[100] S. Dapprich, G. Frenking, J. Phys. Chem. 99 (1995) 9352.
[101] P. Schwerdtfeger, P.D.W. Boyd, A.K. Burrell, W.T. Robinson, M.J. Taylor, Inorg. Chem. 29 (1990) 3593.
[102] P. Pekka, Angew. Chem. Int. Ed. 43 (2004) 4412.
[103] P. Pyykko, N. Runeberg, Chem. Asian J. 1 (2006) 623.
[104] D.J. Gorin, F.D. Toste, Nature 446 (2007) 395.
[105] M.K. Samantaray, V. Katiyar, D. Roy, K. Pang, H. Nanavati, R. Stephen, R.B. Sunoj, P. Ghosh, Eur. J. Inorg. Chem. (2006) 2975.
[106] L. Ray, M.M. Shaikh, P. Ghosh, Inorg. Chem. 47 (2008) 230.
[107] M.K. Samantaray, K. Pang, M.M. Shaikh, P. Ghosh, Inorg. Chem. 47 (2008) 4153.
[108] J.M. Hayes, M. Viciano, E. Peris, G. Ujaque, A. Lledos, Organometallics 26 (2007) 6170.
[109] V.M. Ho, L.A. Watson, J.C. Huffman, K.G. Caulton, New J. Chem. 27 (2003) 1446.
[110] J.C. Garrison, R.S. Simons, W.G. Kofron, C.A. Tessier, W.J. Youngs, Chem. Commun. (2001) 1780.
[111] A.A.D. Tulloch, A.A. Danopoulos, S. Kleinhenz, M.E. Light, M.B. Hursthouse, G. Eastham, Organometallics 20 (2001) 2027.
[112] X.L. Hu, Y.J. Tang, P. Gantzel, K. Meyer, Organometallics 22 (2003) 612.
[113] P. Shukla, J.A. Johnson, D. Vidovic, A.H. Cowley, C.D. Abernethy, Chem. Commun. (2004) 360.
[114] C.D. Abernethy, G.M. Codd, M.D. Spicer, M.K. Taylor, J. Am. Chem. Soc. 125 (2003) 1128.
[115] H. Jacobsen, A. Correa, C. Costabile, L. Cavallo, J. Organomet. Chem. 691 (2006) 4350.
[116] R. Tonner, G. Heydenrych, G. Frenking, Chem. Asian J. 2 (2007) 1555.
[117] M. Tafipolsky, W. Scherer, K. Öfele, G. Artus, B. Pedersen, W.A. Herrmann, G.S. McGrady, J. Am. Chem. Soc. 124 (2002) 5865.
[118] L. Mercs, G. Labat, A. Neels, A. Ehlers, M. Albrecht, Organometallics 25 (2006) 5648.
[119] A.B.P. Lever, Inorg. Chem. 30 (1991) 1980.
[120] A.B.P. Lever, Inorg. Chem. 29 (1990) 1271.
[121] M.D. Sanderson, J.W. Kamplain, C.W. Bielawski, J. Am. Chem. Soc. 128 (2006) 16514.
[122] D.M. Khramov, V.M. Lynch, C.W. Bielawski, Organometallics 26 (2007) 6042.
[123] A.T. Termaten, M. Schakel, A.W. Ehlers, M. Lutz, A.L. Spek, K. Lammertsma, Chem. Eur. J. 9 (2003) 3577.
[124] D. Nemcsok, K. Wichmann, G. Frenking, Organometallics 23 (2004) 3640.
[125] R. Dorta, E.D. Stevens, S.P. Nolan, J. Am. Chem. Soc. 126 (2004) 5054.
[126] N.M. Scott, R. Dorta, E.D. Stevens, A. Correa, L. Cavallo, S.P. Nolan, J. Am. Chem. Soc. 127 (2005) 3516.
[127] C.F. Guerra, J.W. Handgraaf, E.J. Baerends, F.M. Bickelhaupt, J. Comput. Chem. 25 (2004) 189.
[128] H. Jacobsen, J. Organomet. Chem. 690 (2005) 6068.
[129] M.K. Samantaray, D. Roy, A. Patra, R. Stephen, M. Saikh, R.B. Sunoj, P. Ghosh, J. Organomet. Chem. 691 (2006) 3797.
[130] L. Gagliardi, C.J. Cramer, Inorg. Chem. 45 (2006) 9442.
[131] A. Kausamo, H.M. Tuononen, K.E. Krahulic, R. Roesler, Inorg. Chem. 47 (2008) 1145.
[132] M. Cases, G. Frenking, M. Duran, M. Solà, Organometallics 21 (2002) 4182.
[133] K. Morokuma, J. Chem. Phys. 55 (1971) 1236.
[134] T. Ziegler, A. Rauk, Theor. Chim. Acta 46 (1977) 1.
[135] T. Ziegler, A. Rauk, Inorg. Chem. 18 (1979) 1558.
[136] T. Ziegler, NATO ASI C 378 (1992) 367.
[137] F.M. Bickelhaupt, E.J. Baerends, Rev. Comp. Chem. 15 (2000) 1.
[138] H. Jacobsen, T. Ziegler, Comment. Inorg. Chem. 17 (1995) 301.
[139] H. Jacobsen, T. Ziegler, J. Am. Chem. Soc. 116 (1994) 3667.
[140] J.A. Martinho Simões, J.L. Beauchamp, Chem. Rev. 90 (1990) 629.
[141] A. Rosa, G. Ricciardi, E.J. Baerends, J. Phys. Chem. A 110 (2006) 5180.
[142] K. Kitaura, K. Morokuma, Int. J. Quantum Chem. 10 (1976) 325.
[143] H. Fujimoto, Y. Osamura, J. Minato, J. Am. Chem. Soc. 100 (1978) 2954.
[144] P.J. van den Hoek, A.W. Kleyn, E.J. Baerends, Comments At. Mol. Phys. 23 (1989) 93.
[145] T. Ziegler, V. Tschinke, A. Becke, J. Am. Chem. Soc. 109 (1987) 1351.
[146] T. Ziegler, V. Tschinke, C. Ursenbach, J. Am. Chem. Soc. 109 (1987) 4825.
[147] P.S. Bagus, K. Herrmann, C.W. Bauschlicher Jr, J. Chem. Phys. 80 (1984) 4378.
[148] P.S. Bagus, F. Illas, J. Chem. Phys. 96 (1992) 8962.
[149] H.-B. Kraatz, H. Jacobsen, T. Ziegler, P.M. Boorman, Organometallics 12 (1993) 76.
[150] H. Jacobsen, M.J. Fink, Inorg. Chim. Acta 360 (2007) 3511.
[151] H. Jacobsen, H. Berke, S. Doring, G. Kehr, G. Erker, R. Fröhlich, O. Meyer, Organometallics 18 (1999) 1724.
[152] W.A. Herrmann, J. Schutz, G.D. Frey, E. Herdtweck, Organometallics 25 (2006) 2437.
[153] N.P. Mankad, T.G. Gray, D.S. Laitar, J.P. Sadighi, Organometallics 23 (2004) 1191.
[154] T. Ramnial, C.D. Abernethy, M.D. Spicer, I.D. McKenzie, I.D. Gay, J.A.C. Clyburne, Inorg. Chem. 42 (2003) 1391.
[155] C. Bohler, D. Stein, N. Donati, H. Grutzmacher, New J. Chem. 26 (2002) 1291.
[156] D.S. Laitar, P. Muller, T.G. Gray, J.P. Sadighi, Organometallics 24 (2005) 4503.
[157] M.V. Baker, P.J. Barnard, S.K. Brayshaw, J.L. Hickey, B.W. Skelton, A.H. White, Dalton Trans. (2005) 37.
[158] S. Caddick, F.G.N. Cloke, P.B. Hitchcock, A.K.D. Lewis, Angew. Chem. Int. Ed. 43 (2004) 5824.
[159] R. Jackstell, M.G. Andreu, A. Frisch, K. Selvakumar, A. Zapf, H. Klein, A. Spannenberg, D. Rottger, O. Briel, R. Karch, M. Beller, Angew. Chem. Int. Ed. 41 (2002) 986.
[160] R. Dorta, E.D. Stevens, C.D. Hoff, S.P. Nolan, J. Am. Chem. Soc. 125 (2003) 10490.
[161] I.E. Markò, S. Sterin, O. Buisine, R. Mignani, P. Branlard, B. Tinant, J.P. Declercq, Science 298 (2002) 204.
[162] G. Huttner, W. Gartzke, Chem. Ber. 105 (1972) 2714.
[163] K. Abdur-Rashid, T. Fedorkiw, A.J. Lough, R.H. Morris, Organometallics 23 (2004) 86.
[164] W.A. Herrmann, M. Elison, J. Fischer, C. Kocher, G.R.J. Artus, Chem. Eur. J. 2 (1996) 772.
[165] Y. Yamaguchi, R. Oda, K. Sado, K. Kobayashi, M. Minato, T. Ito, Bull. Chem. Soc. Jpn. 76 (2003) 991.
[166] W.A. Herrmann, L.J. Goossen, G.R.J. Artus, C. Kocher, Organometallics 16 (1997) 2472.
[167] M. Niehues, G. Kehr, R. Fröhlich, G. Erker, Zeitschrift fur Naturforschung B 58 (2003) 1005.
[168] A.S. Goldman, K. Krogh-Jespersen, J. Am. Chem. Soc. 118 (1996) 12159.